SYNTHESIS AND ION SENSING PROPERTIES OF NOVEL BORADIAZAINDACENE DYES

A THESIS SUBMITTED TO
THE GRADUATE SCHOOL OF NATURAL AND APPLIED SCIENCES
OF
THE MIDDLE EAST TECHNICAL UNIVERSITY

BY

NALAN ZALİM

IN PARTIAL FULFILLMENT OF THE REQUIREMENTS FOR THE DEGREE OF

MASTER OF SCIENCE

IN

THE DEPARTMENT OF CHEMISTRY

SEPTEMBER 2003

Approval of the Graduate School of Natural and Applied Sciences

_____

Prof. Dr. Canan Özgen
Director

I certify that this thesis satisfies all requirements as a thesis for the degree of Master of Science.

_____

Prof. Dr. Teoman Tinçer
Chairman of the Department

This is to certify that we have read this thesis and in our opinion, it is fully adequate, in scope and quality, as a thesis for the degree of Master of Science.

_____

Prof. Dr. Engin U. Akkaya
Supervisor

Examining Committee Members

Prof. Dr. İdris M. Akhmedov _____

Prof. Dr. İnci Gökmen _____

Prof. Dr. Engin U. Akkaya _____

Assoc. Prof. Dr. Deniz Üner _____

Assoc. Prof. Dr. Özdemir Doğan _____

ABSTRACT

SYNTHESIS AND ION SENSING PROPERTIES OF NOVEL BORADIAZADACENE DYES

Zalim, Nalan

M. S., Department of Chemistry

Supervisor: Prof. Dr. Engin U. AKKAYA

September 2003, 74 pages

The derivatives of boradiazaindacene (BODIPY) are highly fluorescent dyes which have quantum yields near 1.0. These dyes that have exceptional spectral and photophysical stability as compared to other fluorescent groups are used for several different applications.

The fluorescent sensor molecules for the detection of cations with PET (photoinduced-electron transfer) mechanism in general have been obtained by the differentiation of the BODIPY core. The extension of conjugation over the pyrrole ring shifts the absorption and emission at longer wavelength. Moreover, it is seen that red emission occurs from an ICT (intramolecular-charge transfer) state.

In this study, we designed and synthesized an unsymetrically substituted BODIPY dye series, carrying a cation-sensitive phenylazacrown ether group conjugated to the core, and investigated the ion sensing properties of these compounds. Both aza-crown derivatives displayed selectivity towards Ca(II).

Keywords: Chemosensor, BODIPY, azacrown ether, photoinduced-charge transfer

ÖZ

BORADİAZAİNDASEN BOYARMADDELERİNİN SENTEZİ VE İYON ALGILAYICI ÖZELLİKLERİ

Zalim, Nalan

Yüksek Lisans, Kimya Bölümü

Tez Yöneticisi: Prof. Dr. Engin U. AKKAYA

Eylül 2003, 74 sayfa

Boradiazaindasen (BODIPY) türevleri kuantum verimleri 1.0'e yaklaşan çok parlak floresan boyarmaddelerdir. Diğer floresan gruplarla kıyaslandığında fevkalade spektral ve fotofiziksel kararlılığı olan bu boyarmaddelerin çok farklı uygulama alanları vardır.

Boradiazaindasen (BODIPY) yapısı türevlendirilerek çoğunlukla PET (photoinduced-electron transfer) mekanizmasıyla katyon sinyalleyen molecular algılayıcılar elde edilmiştir. Pirol halkası üzerinden konjügasyonun uzatılması, daha uzun dalga boyunda absorpsiyon ve emisyonu mümkün kılmıştır. Ayrıca kırmızı emisyonun bir ICT (intramolecular-charge transfer) düzeyinden olduğu anlaşılmaktadır.

Bu çalışmada, konjüge olarak ana gruba bağlı katyon algılayıcı fenil-aza-taç eter grup taşıyan, simetrik olmayan, bir boradiazaindasen boyarmadde serisi tasarlayıp sentezlemiş ve iyon algılayıcı özellikleri incelenmiştir. Sonuçlar her iki aza-taç eter türevinin de Ca(II) katyonu için seçicilik gösterdiğini ortaya çıkarmıştır.

Anahtar kelimeler: Moleküler algılayıcı, BODIPY, azataç eter, photoinduced-yük aktarımı.

To my family

ACKNOWLEDGMENTS

I would like to express my sincere thanks to my supervisor Prof. Dr. Engin U. Akkaya for his guidance, support and patience during the course of this research as well as his unlimited knowledge and experience that I have benefited from greatly.

I want to thank to my family for their support, understanding and encouragement.

My gratitude to the NMR technician Fatoş is endless.

I would like to thank to our group members. I can never forget the beautiful friendship in our Lab, B-09 (underground organization).

TABLE OF CONTENTS

LIST OF TABLES

TABLE

LIST OF FIGURES

FIGURES

CHAPTER 1

INTRODUCTION

1.1 Supramolecular Chemistry

Supramolecular chemistry is, in Jean-Marie Lehn's words, "Chemistry beyond the molecule", and its goal is to control over the intermolecular noncovalent bond [1-2].

It is a highly interdisciplinary field of science covering the chemical, physical, and biological features of the chemical species of greater complexity than molecules themselves that are held together and organized by means of intermolecular (non-covalent) binding interactions [3].

Supramolecular chemistry is one of the most vigorous and fast-growing fields of chemical endeavor. Its interdisciplinary nature has brought about wide ranging collaborations between physicists, theorists and computational modelers, crystallographers, inorganic and solid state chemists, synthetic organic chemists, biochemists and biologists. In contrast to molecular chemistry which studies the features of the entities constructed from atoms linked by covalent bonds, supramolecular deals with the complex entities formed by the association of two or more chemical species held together by intermolecular non-covalent forces. The objects of supramolecular chemistry are "supramolecular entities, supermolecules

possessing features as well defined as those of molecules themselves. One may say that supermolecules are to molecules and the intermolecular bond what molecule are to atom and covalent bond" [1, 2, 4]. So, the supermolecule represents the next level of the molecule. Figure 1.1 illustrates this relationship between molecular and supramolecular chemisty in terms of both structures and functions.

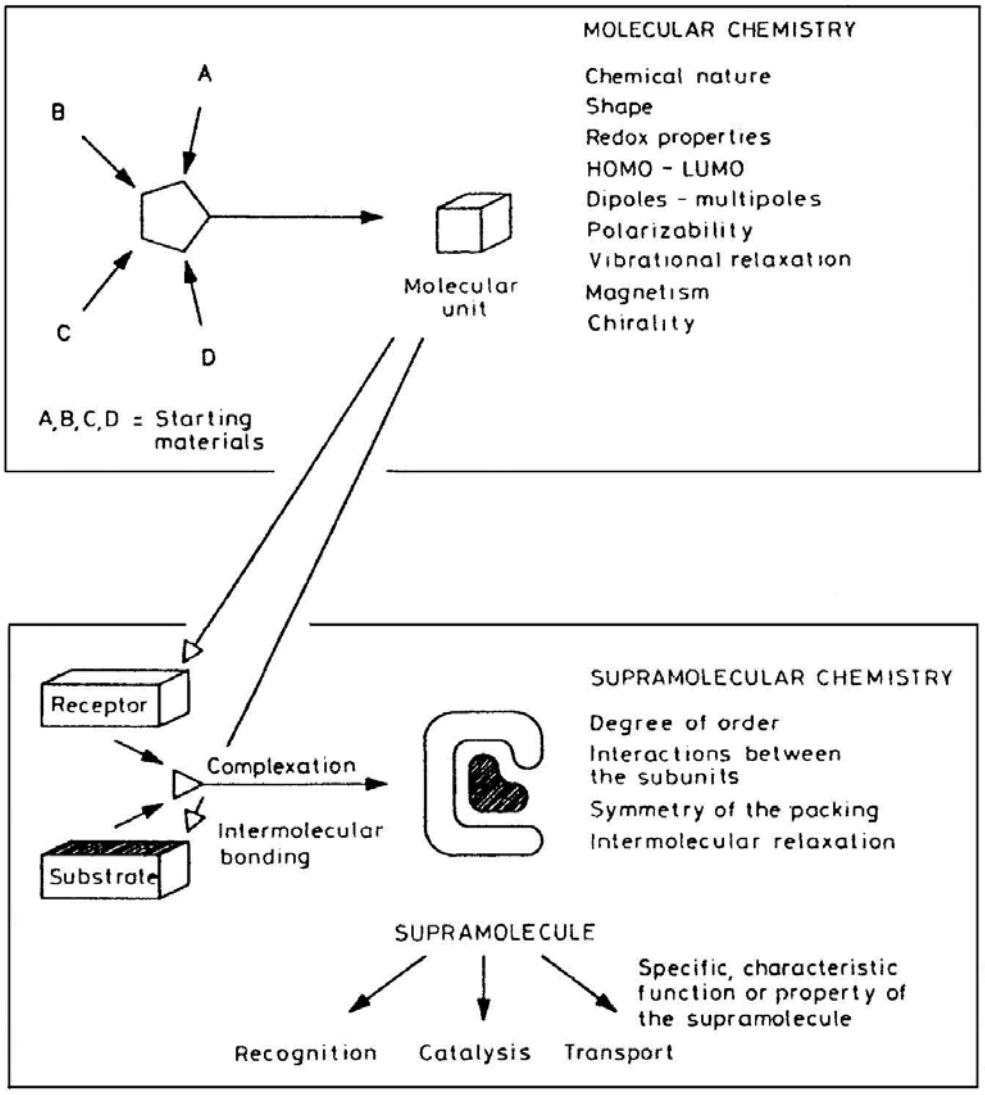

Figure 1.1 From molecular components to supramolecular systems [5].

Nature of Supramolecular Interactions

The non-covalent interactions have a constitutive role in supramolecular structures. The non-covalent interactions involved in supramolecular entities may be a combination of several attractive and repulsive interactions which present different degrees of strength, directionality, dependence of distance and angles, *e.g.* ion-pairing, hydrogen bonding, cation-π, π-π interactions, electrostatic forces, metal ion coordination, donor-acceptor interactions *etc.* Their strengths range from weak or moderate as in hydrogen bonds, to strong or very strong for metal ion coordination. The former responsible for the overall shape of many proteins, recognition of substrates by numerous enzymes, and for the double helix structure of DNA, whereas the latter makes available, by means of a single metal ion binding strengths that lie in the domain of antigen-antibody complexes (or higher), where many individual interactions are involved. All of these interactions are vital for supramolecular systems and effect relating both to the host and guest as well as their surroundings (e.g. solvation, crystal lattice, gas phase etc.).

In contrast to the covalent interactions that dominate in classical molecules, non-covalent interactions are however in general weak interactions that bind together different kinds of building blocks into supramolecular entities. Covalent bonds are generally shorter than 2 Å, while non-covalent interactions function within range of several angstroms. The formation of a covalent bond requires overlapping of partially occupied orbitals of interacting atoms, which share a pair of electrons. In non-covalent interactions, in turn, no overlapping is necessary because the attraction comes from the electrical properties of the building blocks. Because of these weak non-covalent interactions supramolecular species are thermodynamically

less stable, kinetically more labile and dynamically more flexible than molecules.

1.2 A Brief Introduction to Fluorescence

The phenomenon of fluorescence was known by the middle of the nineteenth century. British scientist Sir George G. Stokes first made the observation that the mineral fluorspar exhibits fluorescence when illuminated with ultraviolet light, and he coined the word "fluorescence". Stokes observed that the fluorescing light has longer wavelengths than the excitation light, a phenomenon that has become to be known as the Stokes shift. Fluorescence microscopy is an excellent method of studying material that can be made to fluoresce, either in its natural form or when treated with chemicals capable of fluorescing.

Fluorescence activity can be schematically illustrated with the classical Jablonski diagram, Figure 1.2, first proposed by Professor Alexander Jablonski in 1935 to describe absorption and emission of light.

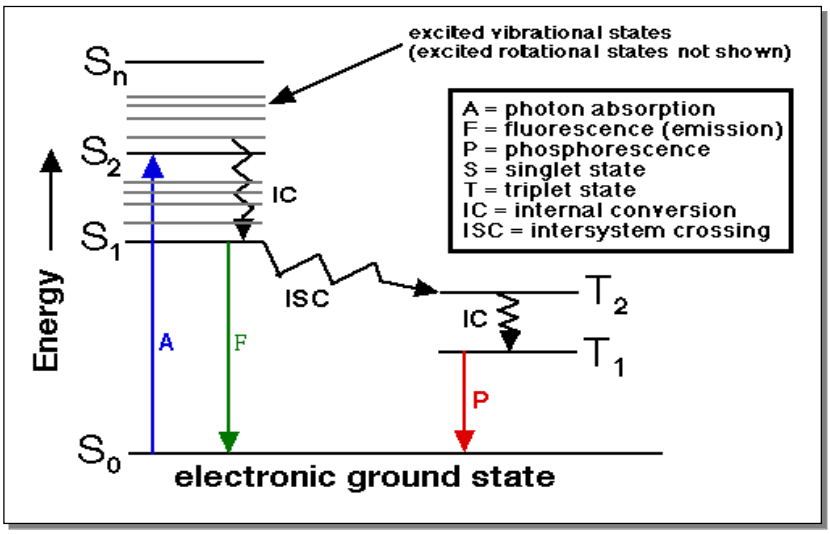

Figure 1.2 Jablonski Diagram [7].

Once a molecule has absorbed energy in the form of electromagnetic radiation, there are a number of routes by which it can return to ground state, one of which is fluorescence. The fluorescence phenomenon may be explained as follows [6];

The absorption of a quantum of light by a molecule results in the elevation of an electron from the molecule's ground electronic state (S_0) to one of several vibrational levels in the electronic excited state. In solution, the excited state molecule rapidly relaxes to the lowest vibrational level of the lowest electronic state (S_1). The energy thus stored in the excited state may be released in several ways. The electron may return to the electronic ground state with only the release of heat (radiationless relaxation). After relaxing thermally to the lowest vibrational level of the S_1 state, the electron may return to the S_0 state with light emission (fluorescence) or, if the molecule is sufficiently long-lived in the S_1 state, it may cross into a lower energy triplet state (T_1) which is named as intersystem crossing (ISC). Relaxation from the T_1 state to the S_0 state can also occur with light emission in solids (phosphorescence), by the release of energy (radiationless transition), or by chemical reaction.

1.2.1 Fluorescence as a Signal Transduction Mechanism

Signal transduction is the mechanism by which an interaction of sensor with analyte yields a measurable form of energy, which can be characterized by various spectroscopies (e.g., UV, visible, NMR) or may yield electrochemical responses [6].

Fluorescence is identified as the optimal signal transduction mechanism in potential sensing applications. There are many reasons for which fluorescence is an

enormously sensitive technique, because the observing wavelength is always longer than that of the exciting wavelength, so that a signal may be read versus zero or near zero background and thus the sensitivity is very high. Owing to the sensitivity of the fluorescence, even low fluorophore levels can be detected. This optical method typically works in the millisecond domain, much faster than the time resolution of other methods. The fluorescence of most biological samples generates background signal up to about 650 nm, in contrast to some applications in which background fluorescence is not a problem. Long wavelength fluorophores (i.e., near-IR) generally avoid these interferences, although sometimes at the cost of severely narrowing the signal transduction mechanisms that function in such compounds. In addition to, fluorescence signaling gives the monitoring of both excitation and emission wavelengths. Fluorescence usually is not destructive so that, fluorescent chemosensors can be used at all levels of organization from whole organs to isolated tissue and can be incorporated into the intact functioning cells without destruction. Fluorescence has the potential for real-time sensing without the need for many steps associated with other analytical methods. Many fluorescent probes have been identified that charge intensity in response to analytes of interest, and more has been synthesized for high specificity and/or sensitivity. Fluorescence signaling can be used in the creation of remote sensing applications with fiber optic techniques. Fiber optic sensors (called optodes) permit wireless communication between the detection element and the analyte, making it particularly attractive for *in situ* remote sensing applications [8-9].

1.3 Molecular Recognition

Molecular recognition is the key component of the emerging science of supramolecular chemistry.

Molecular recognition is defined as the energy and the information engaged in the binding and selection of substrate(s) by a given receptor molecule; it may involve a specific function [10].

Molecular recognition implies the (molecular) storage and (supramolecular) read out of molecular information. The source of information processing at the supramolecular level is represented by molecular recognition events. They may cause changes in electronic, ionic, optical, and conformational properties and so translate themselves into the generation of a signal. Molecular recognition processes may play a role in several key steps: (1) the building up the device from its components; (2) its integration into supramolecular arrangements; (3) the selective operation on given species; (4) the response to external physical or chemical stimuli (light, electrons, ions, molecules, etc.), that may regulate the operation of the device and switch it on or off; (5) the nature of the signals generated and of the signal conversion effected (photon-photon, photon-electron, etc.) [3].

Molecular recognition is involved in many fields such as chemistry, biology, medicine, environment, etc., so that it may be one of the cornerstones of supramolecular chemistry. In particular, selective detection of metal cations involved in biological processes (e.g., sodium, potassium, calcium, magnesium), in clinical diagnosis (e.g., lithium, potassium, aluminum) or in pollution (e.g., lead, mercury, cadmium) has been given substantial attention [11].

There must be large difference between the binding free energies of a given substrate and of the other substrates on account of high recognition by a receptor molecule. With the purpose of achievement large differences in affinity several requirements must be considered [3]:

- *Steric (shape and size) complementarity* between receptor and substrate;
- *Interactional complementarity*, i.e. occurrence of complementary binding sites such as electrostatic, hydrogen bond donor/acceptor, in the correct disposition on substrate and receptor in order to achieve matching electronic and nuclear distribution (electrostatic, H-bonding and van der Waals) maps;
- *Large contact areas* between receptor and substrate;
- *Multiple interaction sites*, in view of the fact that non-covalent interactions are weak than covalent bonds;
- *Strong overall binding*; so as to efficient recognition both high stability and high selectivity, strong binding of receptor and substrate is required;
- *Medium effects* play also an important role through the interaction of solvent molecules with receptor and substrate as well as with each other; hence two partners should present geometrically matched as solvophobic or solvophilic domains.

1.4 Chemosensors

A *sensor* is a device that yields measurable signal in response when interacts with matter or energy. *Chemosensors* are the molecules of abiotic origin that signal the presence of matter of energy [6].

A molecular sensor is composed of signaling unit, receptor and substrate. A receptor portion of the sensor must attract the substrate (guest, analyte). This is the basis of the molecular recognition event, and receptor can be any of the systems, such as crown ethers, cryptands, cavitands and so on. The receptor also be in communication with a signaling unit that is responsive to the guest binding. The signaling unit can yield signal in the different form, e.g., an emission of electromagnetic radiation (photochemical sensing), a current (electrochemical sensing) or an otherwise externally measurable change (e.g. in color or pH).

1.4.1 Fluorescent Chemosensors

A *fluorescent chemosensor* is a molecule of abiotic origin that gives fluorescence signal in response when complexes to an analyte reversibly [6]. Fluorescent sensors undergo photophysical changes (extinction coefficient, fluorescence intensity, shifts in absorption and emission spectra) due to analyte binding.

There are three matters, fundamental to the design of fluorescent chemosensors, which have to be known:

- The way of binding of a molecular entity with selectivity.
- How can one generate signals from such binding processes those are easy to measure?
- The intersect mechanisms for binding and fluorescence signal transduction.

There are some requirements to be satisfied by the fluorescent chemosensors in order to make use of the advantages of them [12-13]:

- The chemosensor must bind the desired analyte selectively as compared to others present in the medium.
- The chemosensor must show sufficient discrimination between the species desired and potential candidates.
- The fluorescence should be as intense as possible; also photostability in the presence of dissolved oxygen is wanted.
- Excitation wavelengths should outnumber 340 nm, due to requirements of expensive quartz rather than glass microscope optics caused from shorter wavelengths; in addition to shorter wavelengths are strongly absorbed by nucleic acids and aromatic amino acids.
- Emission wavelengths should exceed 500 nm to reduce overlap with autofluorescence of some biological samples.
- Toxicity should be minimized.
- There should a large wavelength shift in the excitation or emission spectrum or both that is caused from binding of analyte, so that ratioing of signals at two excitation or two emission wavelengths can be performed [14-15]. Such rationing is extremely precious for getting rid of the irrelevancies such as cell thickness, dye concentration, and wavelength-independent variations in illumination intensity and detection efficiency.
- High extinction coefficients (10^{-3}-10^{-4} M^{-1} cm^{-1}) are necessary for a good signal of the small concentrations of the chemosensor and for ignoring any buffering of ion fluctuations.
- The solubility of the probes in desired medium in which recognition takes place is important. Not only are the water soluble probes but also probes in

organic phase can be desirable, because parameters such as nature of solvent (polarity, hydrogen bonding ability, protic or aprotic character), pH, ionic strength, etc. play a role due to ability of them affecting not only the efficiency and selectivity of binding, but also the photophysical characteristic of the fluorophore.

- Binding to cellular constituents and membranes should be minimized or carefully controlled for specificity. To impermeant through membranes the ability of highly water solubility should be given by adding enough charged polar groups such as carboxylates to the chemosensors, so that once introduced into cells it does not rapidly leak out again. Also these polar groups should be prevented by nonpolar protecting groups removable by cytoplasmic enzymes, so that large populations of cells can be loaded with the indicator by incubating them with the nonpolar membrane-permeant derivative.

1.5 Principles of Fluorescent Chemosensor Design for Cation Recognition

Ion recognition, especially cation recognition, is a subject of reasonable interest because of its implications in many fields: chemistry, biology, medicine, environment, etc. Sodium, potassium, magnesium, calcium are very important cations for some biological processes such as transmission of nerve impulses, regulation of cell activity, constitution in metalloenzymes. Detections of lithium and potassium are vital for the treatment of manic depression and high blood pressure, respectively. Detection of mercury, lead and cadmium is also significant because of

their toxicity for organisms. Fluorescent sensors undergo physical changes, (extinction coefficient, fluorescence intensity, shifts in absorption and emission spectra) as marked as possible upon ion binding [16]. In the design of such sensors, recognition of ions requires special care because attention should be paid to both recognition and signaling moieties. Such fluorescent sensors are named as the fluoroionophore that are composed of a fluorophore and ionophore (receptor) linked to each other, Figure 1.3. The signaling moiety acts as signal transducer, i.e. it converts the formation (recognition event) into an optical signal expressed as the changes in the photophysical characteristics of the fluorophore. These fluorescent sensors are two types with respect to the kind of the linkage of flourophore and receptor. These are conjugate chemosensor and intrinsic chemosensor. In the conjugate chemosensor the receptor is linked to the fluorophore via spacer, however in the intrinsic chemosensor some atoms and groups participating in the complexation belong to the fluorophore. In the structure more than one ionophore and/or more than one fluorophore can present. The connection between the receptor and fluorophore is a very important aspect of fluorescent chemosensor design since the strongest perturbation of the photophysical properties of the fluorophore by the ion is desired.

For designing of fluorescence chemosensors for cations, there are an enormous number of factors that should be paid attention, some of which are listed below:

- Size match between cation and host (receptor) cavity;
- Electrostatic charge;
- Solvent (polarity, hydrogen bonding and coordinating ability);
- Size match between cation and host (receptor) cavity;

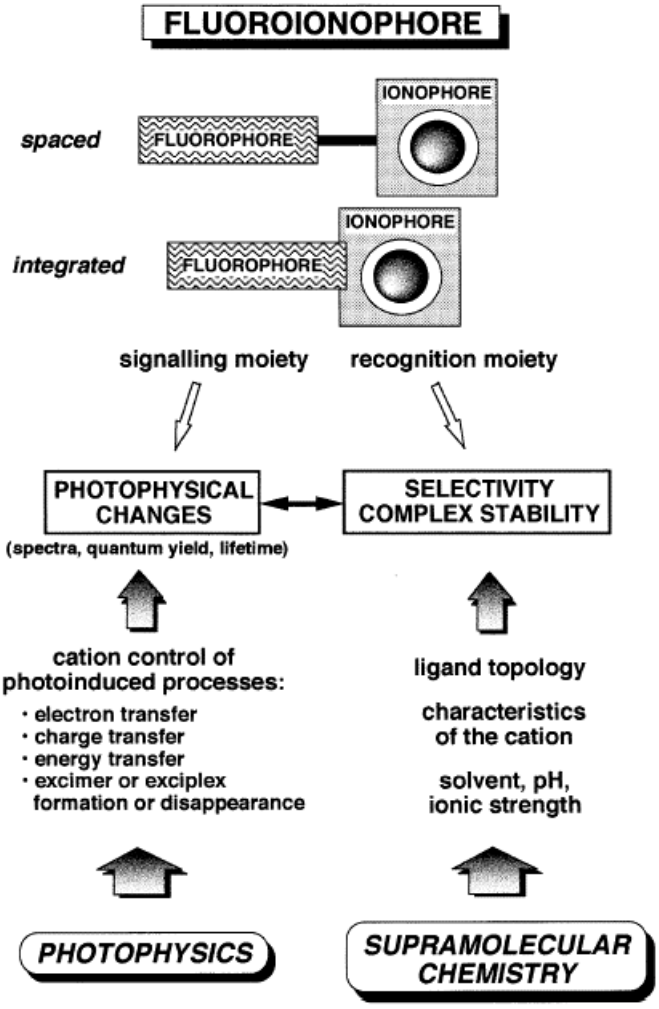

Figure 1.3 Main aspects of fluorescent molecular sensors for cation recognition [17].

- Degree of host preorganization;
- Enthalpic and entropic contributions to the cation-host interaction;
- Cation and host free energies of salvation;
- Nature of the counter-anion and its interactions with solvent and the cation;
- Cation binding kinetics;
- Chelate ring size.

The photophysical changes of a fluorescent probe on recognition should be as marked as possible. Probes undergoing shifts of emission and/or excitation spectra (or appearance or disappearance of bands) are preferable to those that undergo only changes in fluorescence intensity: indeed, after calibration the ratio of the fluorescence intensities at two appropriate emission and excitation wavelengths provides a measure of the ion or molecule concentration which is independent of the probe concentrations (provided that the ion is in excess) and is insensitive to intensity of incident light, scattering, inner-filter effects, and photobleaching [18].

The photophysical changes of a fluorescent chemosensor during interaction with analyte can involve various photoinduced processes, such as energy transfer, excimer or exciplex formation or disappearance, twisted intramolecular charge transfer, etc., but the most important two of them are:

- Photoinduced Electron Transfer (PET)
- Photoinduced Charge Transfer (PCT)

1.5.1 Fluorescent Photoinduced Electron Transfer (PET) Cation Sensors

Fluorescent PET sensors can be formalized as 'fluorophore-spacer-receptor' systems of modular structure [19]. The fluorescent PET sensors also named as intrinsic chemosensors in which the ligand is an integral part of fluorophore π-system. It is well-established that fluorescence signal to be obtained using such probes is stronger and/or more information by creating a different absorbing species on metal ion binding, enabling rationing of the emission signals thereby cancelling

concentration dependent artifacts [20]. To make arrangements for various excitation/emission wavelengths and for a variety of a given guest, the photon- and guest-interaction sites can be chosen. This choice has several constraints; however for the design logic of fluorescent PET sensors these constraints are very important. The energy stored in the fluorophore excited state upon photon absorption must be sufficient to oxidize the guest-free receptor and to simultaneously reduce the fluorophore [21-22]. This is the thermodynamic criterion for a PET sensor, but if the cationic guest is considered it is easy to inhibit the PET process since the oxidation potential of the guest occupied receptor is considerably higher than that of the guest-free receptor. The excited state energy of the optically pumped fluorophore thus remains unused and return as a photon. In the PET sensors the spacer maintains the modularity of the system, which results in the additivity of component parameters, and is only violated by relatively long range forces [23-24].

Figure 1.4 illustrates how a cation can control the photoinduced electron transfer (PET) in a fluoroionophore in which the cation receptor is an electron donor (e.g. amino group) and the fluorophore plays the role of an acceptor. Upon excitation of the fluorophore, an electron of the highest occupied molecular orbital (HOMO) is promoted to the lowest unoccupied molecular orbital (LUMO), which enables PET from the HOMO of the donor (belonging to the free cation receptor) to that of the fluorophore, causing fluorescence quenching of the latter. Upon cation binding, the redox potential of the donor is raised so that the relevant HOMO becomes lower in energy than that of the fluorophore; consequently, PET is not possible any more and fluorescence quenching is suppressed; that means, fluorescence intensity is enhanced upon cation binding [18].

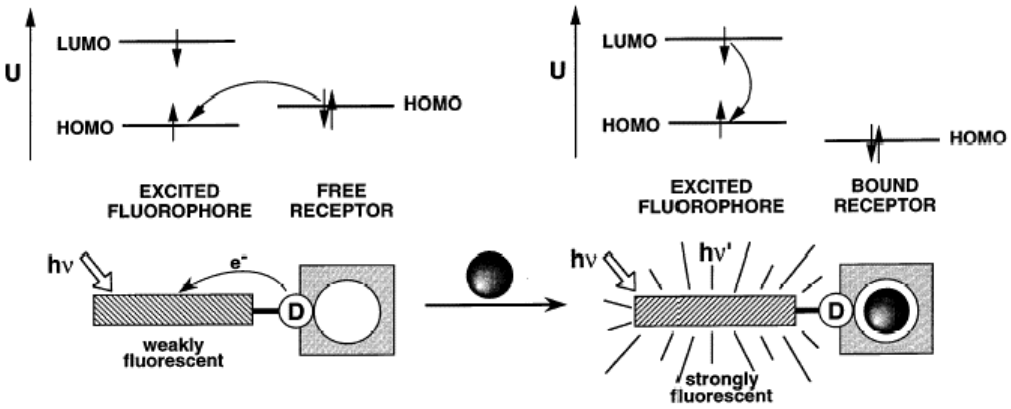

Example:

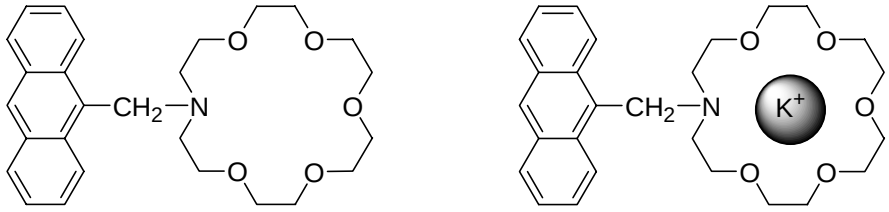

$\Phi_F = 0.003$ (in methanol) $\Phi_F = 0.14$

Figure 1.4 Principle of cation recognition based on cation control of photoinduced electron transfer in nonconjugated donor-acceptor systems [17].
(Example from [25]).

The fluorescence of aromatic hydrocarbons is quenched by aliphatic or aromatic amines due to photoinduced electron transfer from the latter to the former.

In spite of the fact that most PET fluorescent sensors are based on this process, other PET mechanisms can happen with transition metal ions [26-27].

There are various examples of PET sensors some of which are shown in Figure1.5.

PET-1 is the cryptant-based PET sensor. It has beeen successfully used for monitoring levels of potassium in blood and across biological membranes [28]. **PET-2** is the podand-based PET sensor [29-30]. It can bind Cu(II) and Ni(II) and favor oxidation of these cations to the trivalent state. Fluorescence quenching of the anthracene upon binding should be ascribed in this case to an electron transfer from the reducing divalent metal center. **PET-3** is an example of chelating PET sensor. It efficiently binds divalent hard cation of Ca^{2+} [31]. **PET-4** is the calixarene-based PET sensor that is designed for selective recognition of Na^{+}. It contains four carbonyl functions that bind Na^{+}. Complexation with Na^{+} prevents close approach of pyrene and nitrobenzene and thus reduces the probability of PET. The fluorescence quantum yield increases from 0.0025 to 0.016 [32]. **PET-5** is the PET sensor involving excimer formation. There is a large change in the monomer/excimer ratio because of cation binding. There is a concomitant increase in the overall fluorescence emission as a result of the reduction of PET from the nitrogen atom to the phenyl groups. Among the investigated metal ions, the larger stability constants of the complexes were obtained for K^{+} and Ba^{2+}, in accordance with the size of these cations with respect to the crown diameter [33].

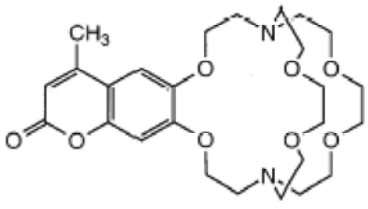

PET-1

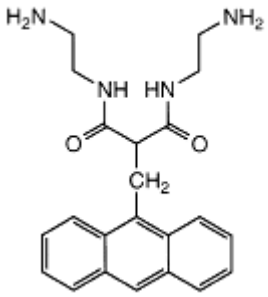

PET-2

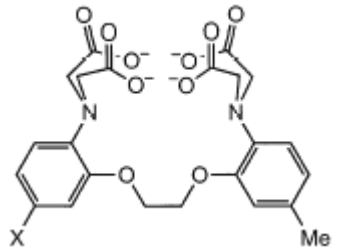

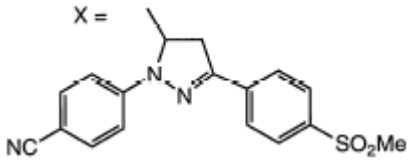

PET-3

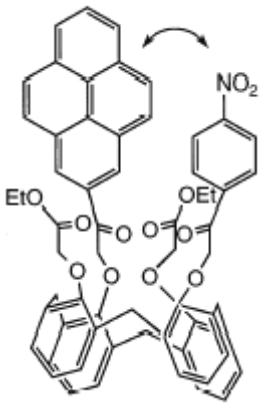

PET-4

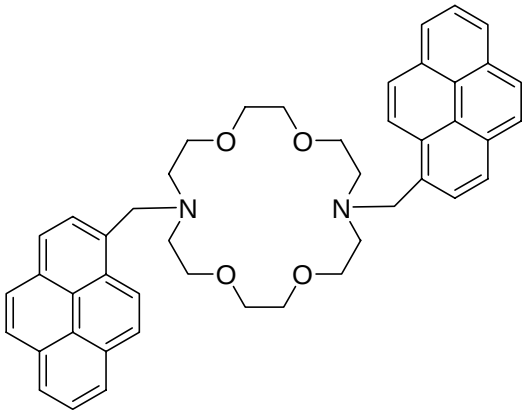

PET-5

Figure 1.5 Some examples of fluorescent PET sensors for various cations**.**

1.5.2 Fluorescent Photoinduced Charge Transfer (PCT) Cation Sensors

A fluorescent PCT sensor contains an electron-donating group (often an amino group) conjugated to an electron-withdrawing group. Upon excitation by light, the PCT sensor undergoes intramolecular charge transfer from the donor to the acceptor; so that a change in dipole moment can occur. This change results in a Stokes shift that depends on the micro environment of the fluorophore. If cations interact closely with the donor or the acceptor moiety of the fluorophore, photophysical properties of the fluorophore will change, because the complexed cation affects the efficieny of the intramolecular charge transfer [16-18].

Interaction of an electron donor group (like an amino group) within fluorophore with a cation causes the reduction of the electron-donating character of this group. A blue shift of the absorption spectrum and a decrease of the extinction coefficient are expected because of the resulting reduction of conjugation. On the other hand, an interaction of a cation with the acceptor group enhances the electron-withdrawing character of this group; as a result that the absorption spectrum is red-shifted and molar absorption coefficient is increased. The fluorescence spectra are in principle shifted in the same direction as those of the absorption spectra. Besides of these shifts, changes in quantum yields and lifetimes are often observed. All these photophysical effects are noticeably dependent on the charge and the size of the cation and selectivity of these effects are expected.

The photophysical changes upon cation binding can also be described in terms of charge dipole interaction [34]. Let us consider only the case where the

dipole moment in the excited state is larger than that in the ground state. Then, when the cation interacts with the donor group, the excited state is more strongly destabilized by the cation than the ground state, and a blue shift of the absorption and emission spectra is expected. Conversely, when the cation interacts with the acceptor group, the excited state is more stabilized by the cation than the ground state, and this leads to a red shift of the absorption and the emission spectra, Figure 1.6.

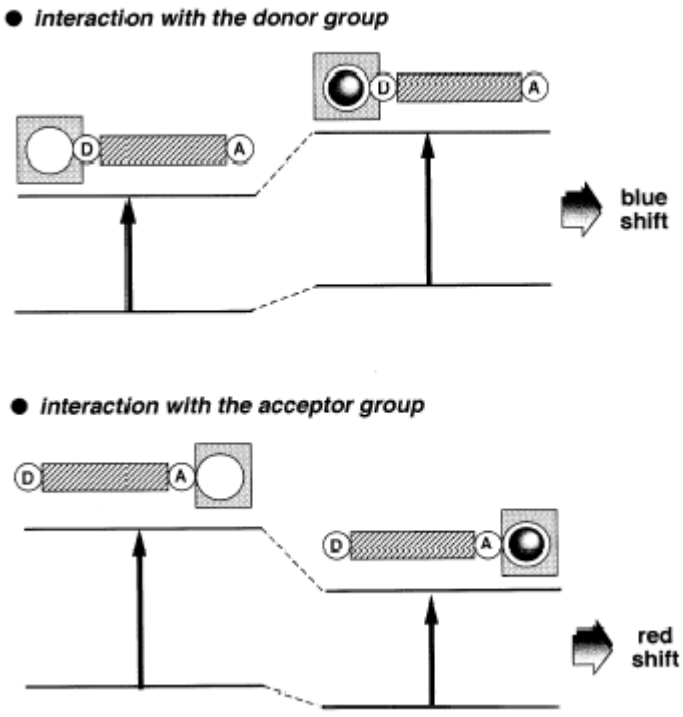

Figure 1.6 Spectral displacements of PCT sensors resulting from interaction of a bound cation with an electron-donating or electron-withdrawing group [17].

Some examples of fluorescent PCT sensors for various cations are given in Figure 1.7.

PCT-1 is one of the first crown-containing fluorescent PCT sensors that have been designed by Valuer. The fluorescence maximum shifts from 642 nm for the free ligand to 574 nm for the Ca^{2+} complex in acetonitrile [35-37]. It is not only responsive to alkaline-earth cations but also to divalent heavy metal ions Hg^{2+} and Pb^{2+} [38]. **PCT-2** shows selectivity for K^{+}. The oxygen atom of the methoxy substituent of the fluorophore can interact with a cation; binding efficiency and selectivity for potassium are thus better than those of the crown alone [39]. **PCT-3** (Mag-Indo1) is a chelating PCT sensor that is selective for Mg^{2+} [40]. **PCT-4** is a PCT sensor in which the bound cation interacts with an electron-withdrawing group. In the sensor, the carbonyl groups of the two coumarin moieties participate in the complexes. Direct interaction between these groups and the cation explains the high stability of constants and the photophysical changes. In addition to the shifts of the absorption and emission spectra, an interesting specific increase in the fluorescence quantum yield upon binding of K^{+} and Ba^{2+} ions has been observed [41].

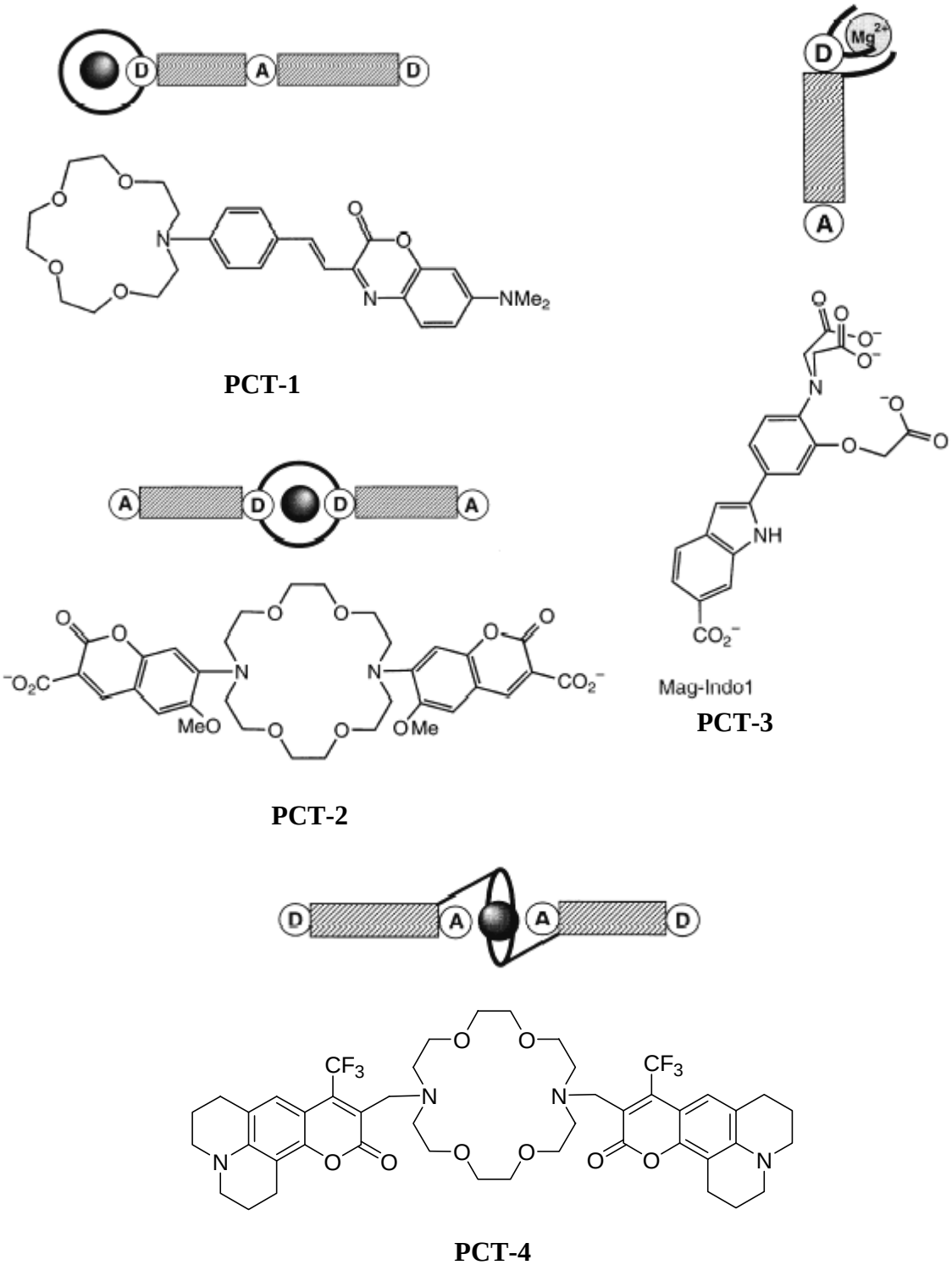

Figure 1.7 Some examples for fluorescent PCT sensors for various cations.

1.6 4,4-Difluoro-4-bora-3a,4a-diaza-*s*-indacene (BODIPY) Dyes

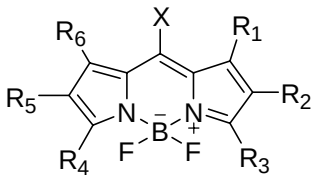

R = H or any group

Figure 1.8 Structure of 4,4-Difluoro-4-bora-3a,4a-diaza-*s*-indacene (BODIPY,BDP).

4,4-Difluoro-4-bora-3a,4a-diaza-*s*-indacene (BODIPY) dyes are highly fluorescent materials that have been used for several different applications. They are currently in use as laser dyes and fluorescent labels for biomolecules and have been incorporated in an electron transfer probe of radical ion pair generated electric fields.

BODIPY dyes combine the advantages of high molar extinction coefficients ($\varepsilon > 70\ 000\ M^{-1}\ cm^{-1}$) and high fluorescence quantum yields (Φ ca. 0.5-0.8) and can be excited at relatively long wavelengths (ca. 500 nm) [42]. These dyes have exceptional spectral and photophysical stability as compared to other fluorescent groups. For example, the commonly used fluorescein exhibits a very similar spectral range as BODIPY, while contrary to BODIPY, the fluorescence and absorption spectra, as well as the fluorescence lifetime, are sensitive to pH and polarity [43].

Up to now, different BODIPY based dyes have been synthesized and their spectroscopic, electrochemical and structural properties have been investigated. The BODIPY dyes **1a-e** and **2a-b**, Figure 1.9, that fluorescence at relatively long

wavelengths were synthesized by Burgess [44]. These dyes have several potential applications. They could aid the design of fluorescent chemosensors, act as receptor molecules for dynamics, structure and function of biomolecules, provide light-harvesting systems for artificial photosynthesis, and for multipigment arrays in molecular photonic devices. The critical difference between structures **1** and **2** is that the former have an aryl group attached to each pyrrole nucleus whereas the latter have only alkyl substituents on that same ring.

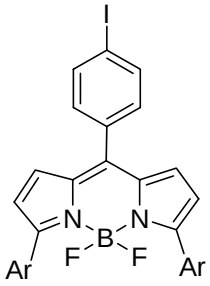

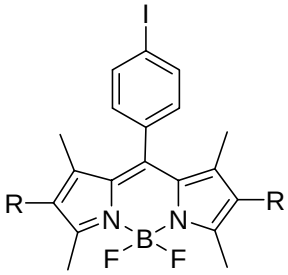

Ar	
1a	Ph
1b	1-Naph
1c	4-$MeOC_6H_4$
1d	4-FC_6H_4
1e	2-$MeOC_6H_4$

R	
2a	H
2b	Et

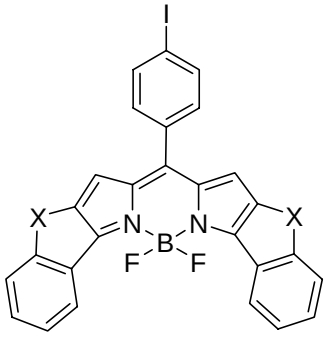

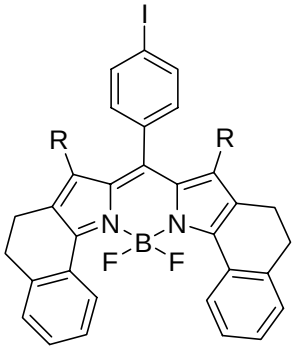

3a	X = O
3b	X = S

4a	R=Y=H
4b	R=H, Y=OMe
4c	R=Me, Y=H

Figure 1.9 Chemical structures of **1a-e**, **2a-b**, **3a-b** and **4a-c.**

UV absorption and fluorescence emission data were compared for compounds **1** and **2**. Absorption and fluorescence emission maxima for compounds **1** occur at higher wavelengths than for compounds **2** because of the added conjugation in compounds **1**, and the Stokes shifts for the aryl-substituted compounds **1** are larger than for the alkyl-substituted compounds **2**. However, the fluorescence quantum yields for the aryl-substituted compounds tend to be lower than the corresponding alkyl-substituted ones which are caused from nonradiative energy loss due to spinning motions about the *C*-aryl single bonds. Also electrochemical properties of these compounds have been investigated by Burgess [44]. These studies demonstrate that electron-withdrawing and electron-releasing aryl substituents have less impact on the oxidation and reduction potentials than expected, consistent with twisting of the aryl substituents out of the BODIPY plane.

The constrained, aryl-substituted BODIPY dyes also have been prepared [45-47]. The planar aromatic compounds **3a-b** and **4a-c**, Figure 1.9, [48] were synthesized and investigated to see if they have more favorable fluorescence characteristics than the unconstrained systems **2**, because molecular constraints are well-known to enhance fluorescence. Dye types **3** and **4** have relatively rigid conformations caused by heteroatom or ethylene bridge linkers that preclude free rotation of the substituted-benzene molecular fragments. In the event, the new types **3** and **4** have longer $\lambda_{max\ abs}$ (620-660 nm) and $\lambda_{max\ fluor}$ (630-680 nm) values than compounds **2**. They also exhibit higher extinction coefficients (> 100 000 M^{-1} cm^{-1}, except for **3b**). Their fluorescent quantum yields are high (up to 0.72 for **4c**), with the exception of compound **3b**.

The BODIPY dyes that show chiral discrimination were synthesized. Compound **5** in Figure 1.10 [49] is the optically active binaphthalene boron-dipyrromethane (BODIPY) which shows chiral discrimination towards the enantiomers of 1-phenylethylamine (PEA) by distinguishable quenching rates of the BODIPY fluorescence. The corresponding plots for the quenching of **5** as a chirally discrimination sensor for optically active amines is shown in Figure 1.11. The steeper slope for quenching with *S*-PEA, based on a higher K_S = 226 M^{-1} for *S*-PEA-**5** as compared to K_S = 161 M^{-1} *R*-PEA-**5,** suggest that association of the *S*-enantiomer and **5** is more efficient. The ratio of $K_S(R\text{-}S)/K_S(R\text{-}R)$ = 1.40 is comparatively high for amine complexes of a simple binaphthol receptor unit in acetonitrile and clearly stress the potential of **5** as an enantioselective sensor molecule.

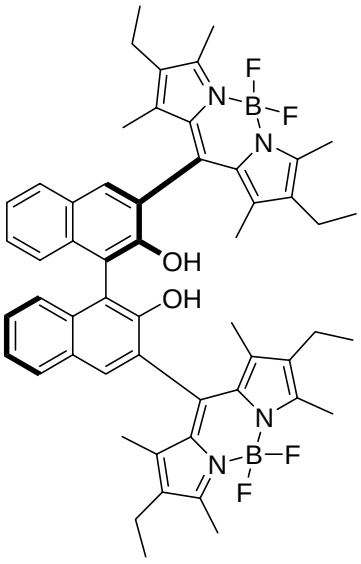

Figure 1.10 Structure of compound **5**.

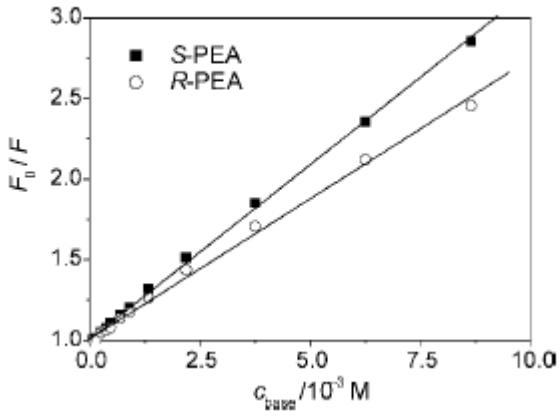

Figure 1.11 Plots for quenching of **5** with *S*-PEA and *R*-PEA in acetonitrile (c_5=5x10^{-6}M, excitation/emission at 490/540nm, *r*=0.999/0.998 for *S*-PEA/*R*-PEA) [49].

The combination of the chiral recognition features of a substituted 1,1'-binaphthalene unit with the favorable spectroscopic properties of the BODIPY chromophore presents a promising approach towards "ON-OFF" signaling of chiral analytes, advantageous both in spectral region and time domain.

The BODIPY based fluorescent chemosensors were designed for anions. For example; the fluorescence emission intensity of the 1:1 Zn(II) complex of a doubly BODIPY substituted bipyridyl ligand is highly sensitive to anion coordination to the metal center which is shown in Figure 1.12, [50].

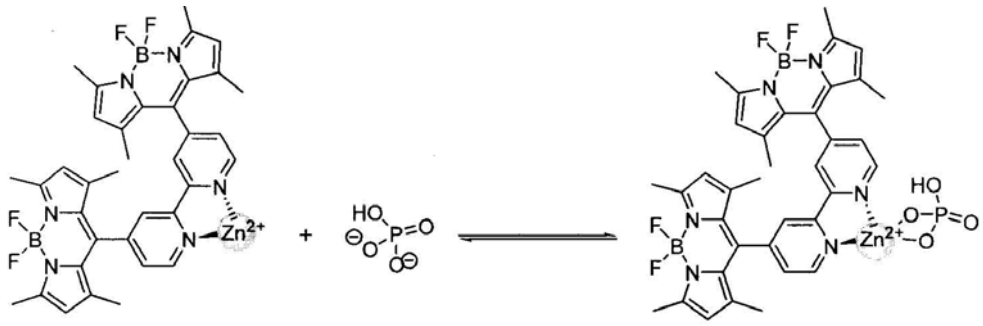

Figure 1.12 The effect of phosphate binding in fluorescence.

BODIPY-Zn(II) complex solution does not give detectable fluorescence emission because one of the most effective quenchers of the fluorescence of the BODIPY compound is Zn(II). However, when phosphate is added, the solution gives bright green fluorescent, because oxidative PET, which is responsible for the quenching of the fluorescence in the complex, is effectively inhibited by anion coordination, leading to a 25-fold enhancement of the emission intensity at 518 nm on phosphate binding which is shown in Figure 1.13.

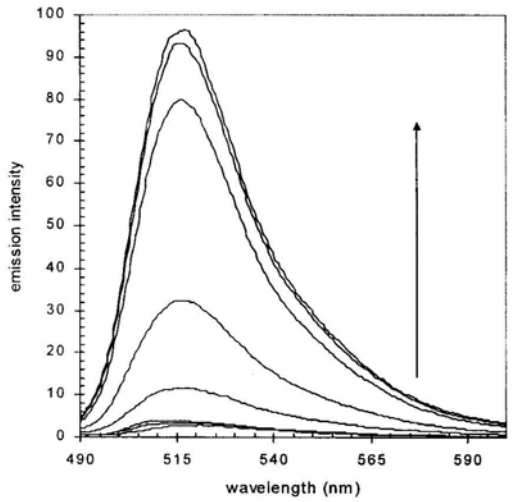

Figure 1.13 Emission spectrum of the Zn(II) complex in response to increasing phosphate concentrations [50].

The spectroscopically advantageous properties and the high electron affinity of the BODIPY fluorophore that promises fast and efficient charge transfer, give a chance to synthesize and investigate the crown ether substituted BODIPY dye **6,** which is shown in Figure 1.14, under the premise of developing new and highly sensitive fluorescent probes for metal ions [42]. In the crowned compound, coordination of the cation to the nitrogen donor atom of the crown inhibits the charge-transfer process, leading to a cation-dependent enhancement of the locally excited state emission and the fluorescence lifetimes by factors > 10^3. This efficient "switching on" of the fluorescence offers the crowned BODIPY dye an extremely sensitive fluorescent probe for metal ions. The complexation of the employed alkali and alkali-earth metal ions leads to FEF (fluorescence enhancement factor) whose size depends on both charge density and the extent of coordination to the crown nitrogen, Figure 1.15. Analysis of the fluorescence titration curves shows that in all the cases studied complexes of a well defined 1:1-stoichiometry were performed,

Figure 1.16. The effect of the complexation on the fluorescence quantum yields is very remarkable, i.e., the chelation-induced FEF vary from 90 for Li^{+} to 2250 for Mg^{2+}, these are the very high fluorescence enhancement values.

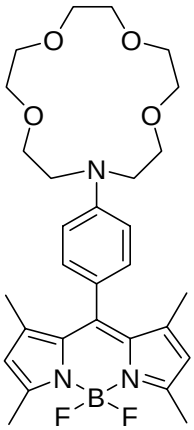

Figure 1.14 Structure of compound **6**.

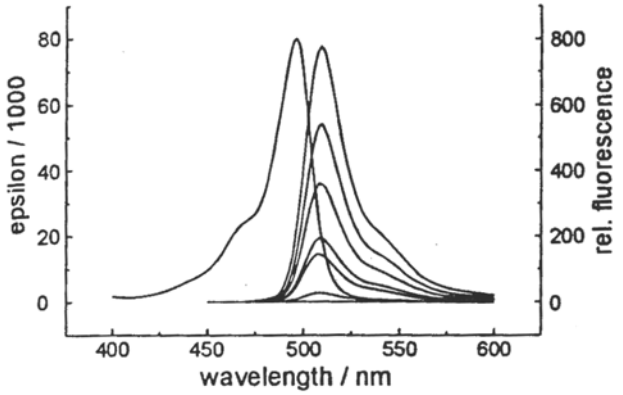

Figure 1.15 Absorption spectra of **6** (left), emission spectra of the complexes with (from top to bottom) Mg^{2+}, Ca^{2+}, Sr^{2+}, Ba^{2+}, Na^{+}, Li^{+} and free ligand in MeCN (excitation at 480 nm) [42].

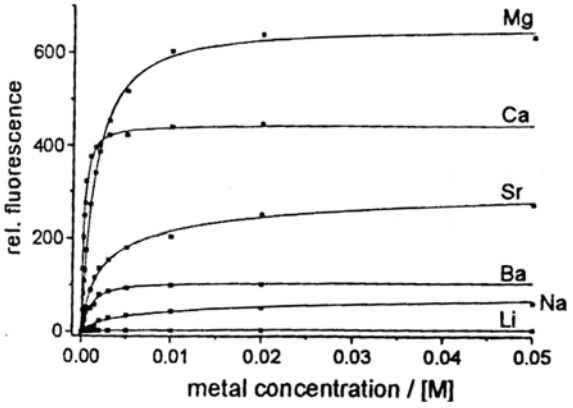

Figure 1.16 Changes in fluorescence intensity of **6** upon addition of metal ions (excitation at 480 nm, detection at 515 nm) in acetonitrile [42].

In addition, thia aza crown substituted BODIPY dye that shows a strong fluorescence enhancement selectively with Hg^{II}, Ag^{I}, and Cu^{II} is synthesized [51].

The BODIPY chromophore has gained an importance in the design of and the constraction of molecular signaling systems capable of performing photo- and substrate-induce logic functions or redox-based switching actions since the BODIPY core is comparatively readily oxidized and reduced, a prerequisite for fluorescent switches relying on electron or charge transfer, as well as for the generation of stable radical ions that show electrogenerated chemiluminescence upon charge recombination. In these systems, the *meso*-substituted BODIPY chromophore acts as in donor(D)-acceptor(A)-substituted biaryls. For example; compound **7** which is shown in Figure1.17 exhibits efficient on/off switching of emission triggered by protonation/deprotonation process in chloroform [52-53].

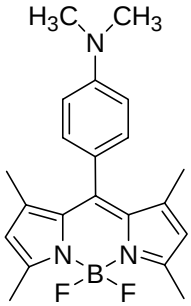

Figure 1.17 Structure of compound **7**.

Protonation of the dimethylamino donor leads to an increase of its oxidation potential, and this loss of donor properties re-establishes fluorescence as the major deactivation route for the S_1 state. The compound represents an excellent PET pH indicator, because; (a) only fluorescence intensity is proton-controlled, whereas all

other spectral parameters are pH invariant, (b) it has very high photostability, (c) high fluorescence quantum yield, and (d) long excitation wavelength which make the sensor excitable by inexpensive blue-green light-emitting diodes.

In addition to *meso*-substituted BODIPY chromophores, there are more advanced molecular ensembles that generate signal changes by substrate interaction at a site conjugated to the BODIPY core. Therefore, dye **8** that is an unsymetrically substituted BODIPY dye carrying an analyte-sensitive (donor) group conjugated to the core was synthesized, Figure 1.18, [54].

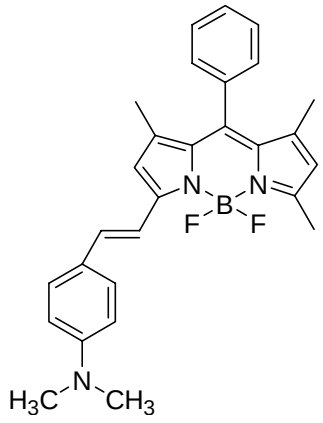

Figure 1.18 Structure of compound **8**.

This dye is a multifunctional molecular system that can either be utilized for highly sensitive probing of solvent polarity and acidity through measuring fluorescence or can be employed as an efficient dual-mode chemical (protons)/electrochromic switch in the red/NIR, operating already at very low voltages. As follows from Table 1, the absorption shows no solvent dependency, whereas the fluorescence of the **8** is strongly dependent on the polarity of the solvent that is the indicative of an intramolecular-charge transfer (ICT) process.

Table 1. Spectroscopic data of **8** and **8**-H^+ in different solvents at 298 K[a] [54].

	Solvent	λ_{abs} [nm]	ε_{max} [$M^{-1}cm^{-1}$]	λ_f [nm]	Φ_f	τ_f [ns]	k_f[b] [$10^8 s^{-1}$]	k_{nr}[b] [$10^8 s^{-1}$]
1	MeCN	597	75000	731	0.13	0.94	1.4	9.2
1	THF	603	89000	672	0.58	3.21	1.8	1.3
1	Et_2O	594	98000	638	0.83	3.88	2.1	0.4
1	Bu_2O	598	101000	630	0.87	3.73	2.3	0.3
1	hexane	596	n.d.[c]	611	0.97	3.84	2.5	0.1
1-H^+	MeCN	553	100000	563	0.97	4.38	2.2	0.1
1-H^+	THF	558	100000	566	0.85	4.02	2.1	0.3
1-H^+	Et_2O	556	101000	563	0.90	4.24	2.1	0.2

[a] Experimental conditions: c(**8**) = $1x10^{-6}$ M, λ_{exc}= 545 and 595 nm for steady-state, 500 and 578 nm for time-resolved fluorescence measurements, proton source $HClO_4$. [b] $k_f = (1-\Phi)/\tau_f$. [c] Not determined due to low solubility.

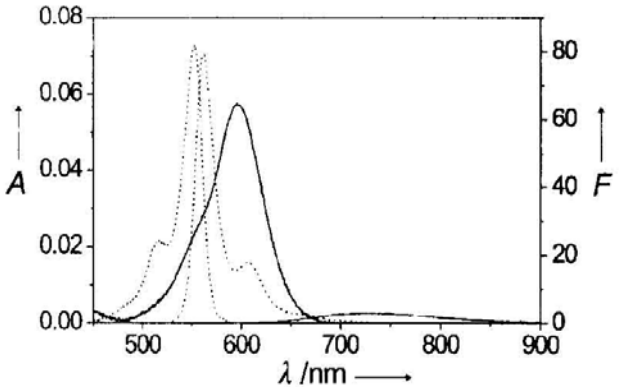

Figure 1.19 Steady-state spectra of **8** (——) and **8**-H^+ (.....) in acetonitrile at 298 K (the emission spectra are normalized at the same optical density at the excitation wavelength 545 nm, experimental conditions are given in Table 1), [54].

Protonation drastically alters the electron-donating properties of the dimethylamino group and consequently "switches off" any charge transfer interaction. This result in typical BODIPY like narrow, structured and solvent-polarity-independent absorption and emission bands, Figure 1.19, the latter of high fluorescence yield in all the acidified solvents employed. The absorption bands of **8**-H^+ are blue-shifted

by about 40 nm compared to those of **8**, and the width of the band is further reduced, stressing the influence of the conjugated (unprotonated) dimethylamino substituent on the spectroscopic properties of **8** in solvents any polarity.

1.7 Aim of the Study

Our aim in this thesis study is to synthesize and investigate the ion sensing properties of novel boradiazaindacene dyes.

We have synthesized a series of BODIPY based dyes carrying a cation-sensitive phenylazacrown ether group conjugated to the polymethinic part of the chromophore. These dyes are the examples for efficient CT (charge transfer) systems in which the extension of the conjugation over the pyrrole ring shifts the absorption and emission to longer wavelength. These chemosensors are expected to generate signal changes by metal ion complexation and protonation. With this study, we present a new design concept for sensitive probes for metal ions showing absorption and fluorescence changes in the red/NIR. We expect this project to open a new path for the synthesis and development of novel sensors of cations in different media, which require red to near-IR excitation and emission. Such an cation chemosensor would be very valuable in studying various biological phenomena.

CHAPTER 2

EXPERIMENTAL

2.0 Instrumentation

In this study, the compounds are characterized by Nuclear Magnetic Resonance technique. ^{1}H and ^{13}C-Nuclear Magnetic Resonance spectra were recorded on a Bruker Instruments Avance Series-Spectropin DPX-400 Ultra shield (400 MHz) High Performance digital FT-NMR Spectrometer (METU NMR Laboratory by using $CDCl_3$ as solvent and chemical shifts δ in ppm from tetramethylsilane as an internal reference). Spin multiplicities are indicated by the following symbols: s (singlet), d (doublet), t (triplet), m (multiplet).

Electronic absorption spectra were recorded on a Shimadzu UV-1601 spectrophotometer. A Perkin-Elmer LS 50 B luminescence spectrometer was used for recording the fluorescence-emission spectra. The emission was detected with a Hamamatsu R928 PMT. All instrumental parameters were controlled by Fluorescence Data Manager Software (FLDM). Measurements were conducted at 25ºC using a 1x0.5 cm rectangular quartz cuvette.

Column chromatography was performed using Merck Silica Gel 60 (particle size:0.040-0.0963, 230-400 mesh ASTM). All reactions were monitored by thin

layer chromatography using Merck Silica Gel 60 F_{254} TLC Aluminum Sheets 20x20cm. All chemicals and solvents purchased from Aldrich Chemical Company unless otherwise stated.

2.1 Synthesis of 16-(4-Propenyl-phenyl)-1,4,7,10,13-pentaoxa-16-aza-cyclooctadecane Substituted BODIPY Dye (8)

2.1.1 Synthesis of 16-Phenyl-1,4,7,10,13-pentaoxa-16-aza-cyclooctadecane (3)

A two-necked, N_2-flushed flask was purged with N_2. NaH (60% in mineral oil, 0.42 g, 0.0175 mol) was added to the reaction vessel and washed 4 times with 50 mL hexane. THF (25 mL) and then 2-[(2-Hydroxy-ethyl)-phenyl-amino]-ethanol **(1)** (1.53 g, 0.01 mol) was added to the flask. The suspension was heated to reflux with vigorous stirring. A solution of the tetra(ethylene glycol)di-*p*-tosylate **(2)** (5.03 g, 0.01 mol) in THF (10 mL) was added dropwise. Reflux was continued for 20 h. The reaction mixture was cooled and quenched with H_2O, and then extracted with CH_2Cl_2 (3x100 mL). The combined organic layers were dried over Na_2SO_4 and concentrated under reduced pressure. The desired product was purified by silica gel column chromatography ($CHCl_3$/methanol 94:6). Further purification was achieved by subsequent column purifications ($CHCl_3$/methanol 94:6) when necessary. The yield of **(3)** was 350 mg (10%).

^{1}H-NMR δ 3.55 (m, 4H), 3.59-3.74 (m, 16H), 3.79 (m, 4H), 6.70 (m, 3H), 7.20 (m, 2H), (Figure A.1).

^{13}C-NMR δ 52.40, 56.31, 61.42, 69.43, 70.71, 70.86, 112.80, 117.00, 129.63, 148.35, (Figure A.2).

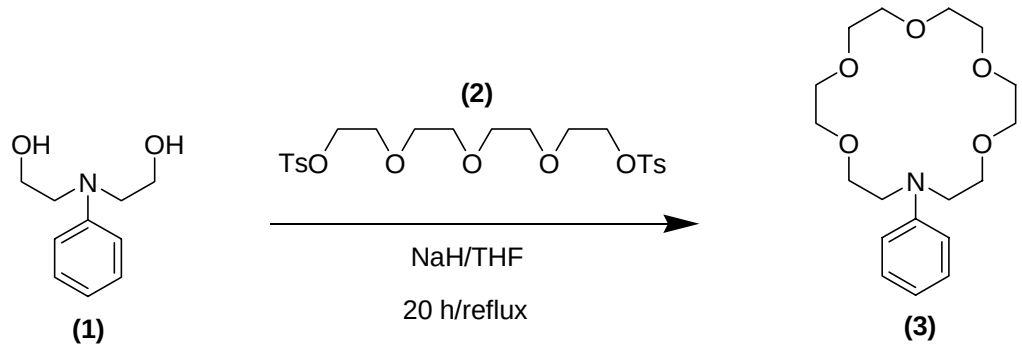

Figure 2.1 Synthesis of 16-Phenyl-1,4,7,10,13-pentaoxa-16-aza-cyclooctadecane **(3)**

2.1.2 Synthesis of 4-(1,4,7,10,13-Pentaoxa-16-aza-cyclooctadec-16-yl)-benzaldehyde (4)

16-Phenyl-1,4,7,10,13-pentaoxa-16-aza-cyclooctadecane **(3)** (100 mg, 0.3 mmol) was dissolved in 2 ml of dimethylformamide. The mixture was cooled in an ice bath and phosphorus oxychloride (46 mg, 0.3 mmol) was added dropwise with stirring, and the reaction mixture was taken from ice bath after 10 min. Then the mixture was stirred at room temperature for 1.5 h, then at 100°C for 3-4 h. The mixture was then cooled and poured over 10 g of crushed ice and stirred for 30 min. The solution was neutralized with 6 M of NaOH solution. The reaction mixture was then extracted with $CHCl_3$ (3x100 mL). The combined organic layers were dried with Na_2SO_4 and concentrated under reduced pressure. The desired product was purified by silica gel column chromatography ($CHCl_3$/methanol 100:7). The yield of **(4)** was 72 mg (65%).

^{1}H-NMR δ 3.43-3.48 (m, 16H), 3.55 (m, 8H), 6.56 (d, 2H, *J*=9.0), 7.53 (d, 2H, *J*=9.0), 9.54 (s, H), (Figure A.3).

^{13}C-NMR δ 51.82, 68.75, 71.15, 71.23, 111.41, 125.64, 132.53, 153.10, 190.49, (Figure A.4).

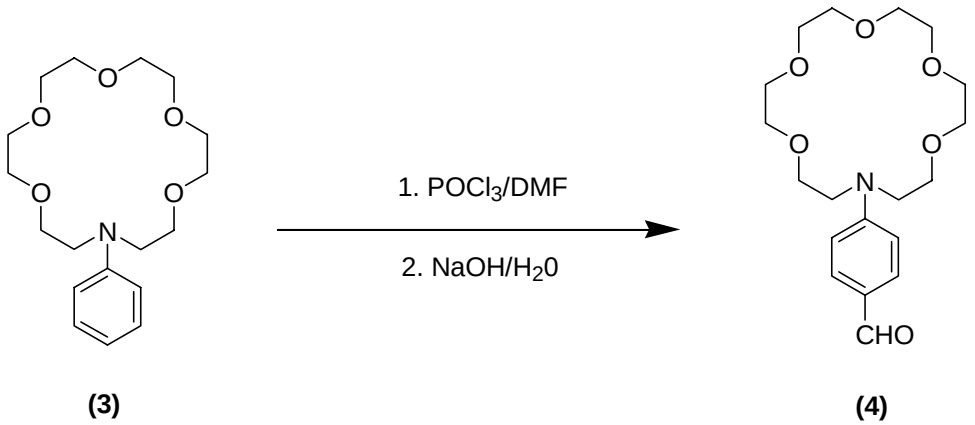

(3) **(4)**

Figure 2.2 Synthesis of 4-(1,4,7,10,13-Pentaoxa-16-aza-cyclooctadec-16-yl)-benzaldehyde **(4)**

2.1.3 Synthesis of 4,4-Difluoro-4-bora-3a,4a-diaza-s-indacene (BODIPY) (7)

The procedure for this reaction is adopted from an earlier report by Rurack [42]. Benzaldehyde **(5)** (0.22 g, 2 mmol) and 2,4-dimethylpyrrole **(6)** (0.38 g, 4mmol) were dissolved in 250 ml of absolute methylene chloride under nitrogen atmosphere. One drop of trifluoroacetic acid was added and the solution was stirred at room temperature until TLC-control (CH_2Cl_2) showed complete consumption of the aldehyde. At this point, a solution of tetrachloro-1,4-benzoquinone (TCBQ) (0.49 g, 2 mmol) in CH_2Cl_2 (100 mL) was added, and stirring was continued for 15 min followed by addition of triethylamine (4 mL) and $BF_3.Et_2O$ (4mL). After stirring for

another 30 min the reaction mixture was washed with water and dried over Na_2SO_4, and solvent was evaporated in *vacuo.* The residue was chromatographed on a silica column (CH_2Cl_2). The yield of **(7)** was 280 mg (0.86 mmol, 43%).

^{1}H NMR δ 1.37 (s, 6H), 2.56 (s, 6H), 5.98 (s, 2H), 7.26-7.30 (m, 2H), 7.47-7.50 (m, 3H), (Figure A.5).

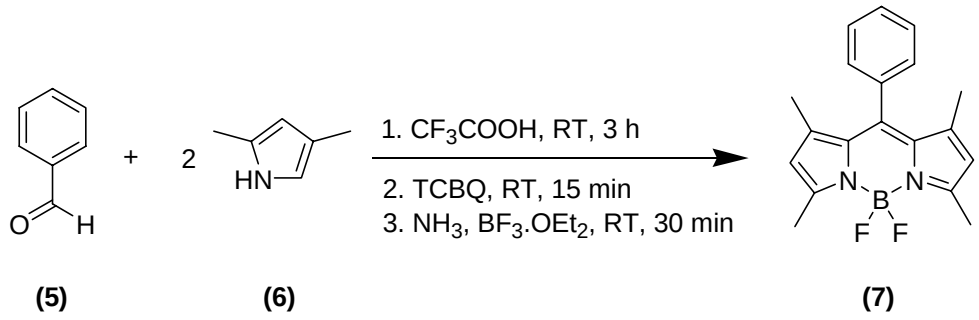

(5) **(6)** **(7)**

Figure 2.3 Synthesis of 4,4-Difluoro-4-bora-3a,4a-diaza-s-indacene (BODIPY) **(7)**

2.1.4 Synthesis of 4,4-Difluoro-4-bora-3a,4a-diaza-*s*-indacene (BODIPY) Dye (8).

4-(1,4,7,10,13-Pentaoxa-16-aza-cyclooctadec-16-yl)-benzaldehyde **(4)** (65 mg, 0.18 mmol) and 4,4-Difluoro-4-bora-3a,4a-diaza-s-indacene (BODIPY) (57 mg, 0.18 mmol) were refluxed for 26 h in a mixture of toluene (5 ml), glacial acetic acid (100 µl, 1.76 mmol) and piperidine (174 µl, 1,76 mmol) together with a small amount of moleculer sieves (4 Å). After cooling to room temperature the mixture was placed on top of a silica column and eluted with ($CHCl_3$/methanol 100/3) and blue fraction is collected. Then PTLC was applied for further purification with ($CHCl_3$/methanol 100/5). The yield was 10 mg (8%).

^{1}H-NMR δ 1.38 (s, 3H), 1.42 (s, 3H), 1.54 (s, 3H), 3.53-3.66 (m, 20H), 3.73 (m, 4H), 5.94 (s, 1H), 6.55 (s, 1H), 6.63 (d, 2H, *J*=8.9), 7.25-7.30 (m, 7H), 7.64 (m, 2H), (Figure A.6).

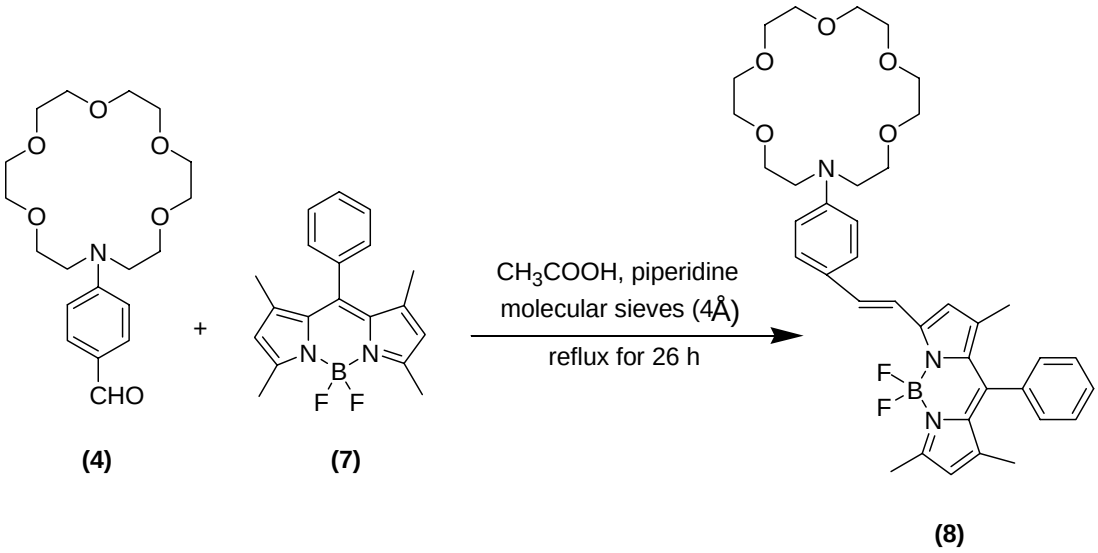

Figure 2.4 Synthesis of 4,4-difluoro-4-bora-3a,4a-diaza-s-indacene (BODIPY) dye **(8)**

2.2 Synthesis of 13-(4-Propenyl-phenyl)-1,4,7,10-tetraoxa-13-aza-cyclopentadecane Substituted BODIPY Dye (12)

2.2.1 Synthesis of 13-Phenyl-1,4,7,10-tetraoxa-13-aza-cyclopentadecane (10)

A two-necked, N_2-flushed flask was purged with N_2. NaH (60% in oil, 0.42 g, 0.0175 mol) was added to the reaction vessel and washed 4 times with 50 mL hexane. THF (25 ml) and then 2-[(2-Hydroxy-ethyl)-phenyl-amino]-ethanol **(1)**

(1.53 g, 0.01 mol) was added to the flask. The suspension was heated to reflux with vigorous stirring. A solution of the tri(ethylene glycol)di-*p*-tosylate **(9)** (4.58 g, 0.01 mol) in THF (10 ml) was added dropwise. Reflux was continued for 20 h. The reaction mixture was cooled and quenched with H_2O, and then extracted with CH_2Cl_2 (3x100 ml). The combined organic layers were dried over Na_2SO_4 and concentrated under reduced pressure. The desired product was purified by silica gel column chromatography ($CHCl_3$/methanol 100:7). Further purifications were achieved by subsequent columns ($CHCl_3$/methanol 100:7) when necessary. The yield of **(10)** was 230 mg (8%).

^{1}H-NMR δ 3.55 (m, 4H), 3.58-3.74 (m, 12H), 3.80 (m, 4H), 6.71 (m, 3H), 7.24 (m, 2H), (Figure A.7).

^{13}C-NMR δ 52.42, 56.34, 69.44, 70.59, 70.70, 116.13, 117.03, 129.65, 148.38, (Figure A.8).

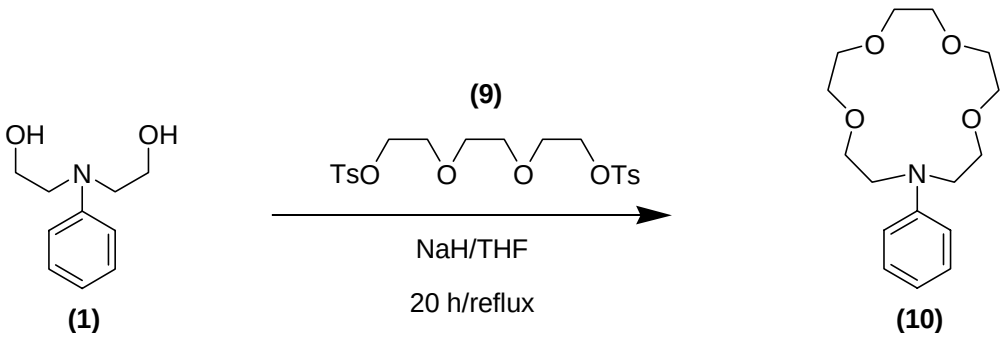

Figure 2.5 Synthesis of 13-Phenyl-1,4,7,10-tetraoxa-13-aza-cyclopentadecane **(10)**

2.2.2 Synthesis of 4-(1,4,7,10-Tetraoxa-13-aza-cyclopentadec-13-yl)-benzaldehyde (11)

13-Phenyl-1,4,7,10-tetraoxa-13-aza-cyclopentadecane **(10)** (100 mg, 0.34 mmol) was dissolved in 3 ml of dimethylformamide. The mixture was cooled in an ice bath and phosphorus oxychloride (52 mg, 0.340 mmol) was added dropwise with stirring, and the reaction mixture was taken from ice bath after 10 min. Then the mixture was stirred at room temperature for 1.5 h, then at 100°C for 3-4 h. The mixture was then cooled and poured over 10 g of crushed ice and stirred for 30 min. The solution was neutralized with 6 M of NaOH solution. The reaction mixture was then extracted with $CHCl_3$ (3x100 ml). The combined organic layers were dried with Na_2SO_4 and concentrated under reduced pressure. The desired product was purified by silica gel column chromatography ($CHCl_3$/methanol 100:7). The yield was 78 mg (71%).

^{1}H-NMR δ 3.62-3.72 (m, 16H), 3.80 (t, 4H, *J*=14.4), 6.75 (d, 2H, *J*=8.9), 7.76 (d, 2H, *J*=8.9), 9.78 (s, H), (Figure A.9).

^{13}C-NMR δ 51.90, 53.78, 68.90, 71.00, 71.14, 111.50, 126.44, 132.60, 152.14, 190.53, (Figure A.10).

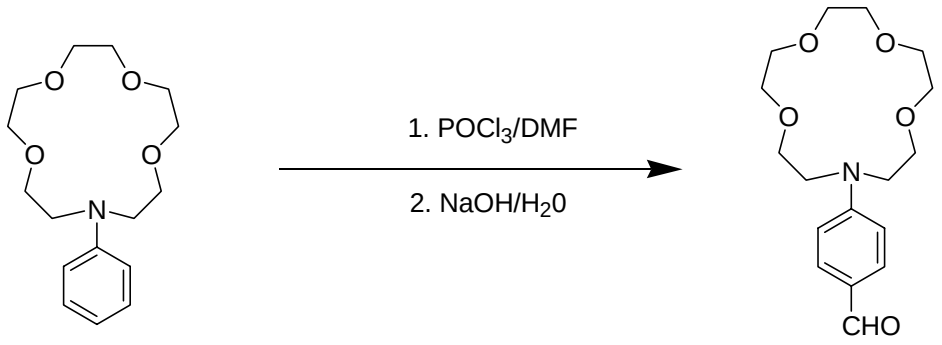

(10) **(11)**

Figure 2.6 Synthesis of 4-(1,4,7,10-Tetraoxa-13-aza-cyclopentadec-13-yl)-benzaldehyde **(11)**

2.2.3 Synthesis of 4,4-Difluoro-4-bora-3a,4a-diaza-*s*-indacene (BODIPY) Dye (12)

4-(1,4,7,10-Tetraoxa-13-aza-cyclopentadec-13-yl)-benzaldehyde **(11)** (65 mg, 0.18 mmol) and 4,4-Difluoro-4-bora-3a,4a-diaza-s-indacene (BODIPY) (57 mg, 0.18 mmol) were refluxed for 26 h in a mixture of toluene (5 ml), glacial acetic acid (100 µl, 1.76 mmol) and piperidine (174 µl, 1,76 mmol) together with a small amount of moleculer sieves (4 Å). After cooling to room temperature the mixture was placed on top of a silica column and eluted with ($CHCl_3$/methanol 100/3) and blue fraction is collected. Then PTLC was utilized to achieve further purification using $CHCl_3$/methanol (100/5). The yield was 6 mg (5%).

^{1}H-NMR δ 1.35 (s, 3H), 1.46 (s, 3H), 1.55 (s, 3H), 3.62-3.72 (m, 16H), 3.80 (m, 4H), 5.90 (s, 1H), 6.51 (s, 1H), 6.59 (d, 2H, *J*=8.9), 7.28-7.32 (m, 7H), 7.54 (d, 2H), (Figure A.11).

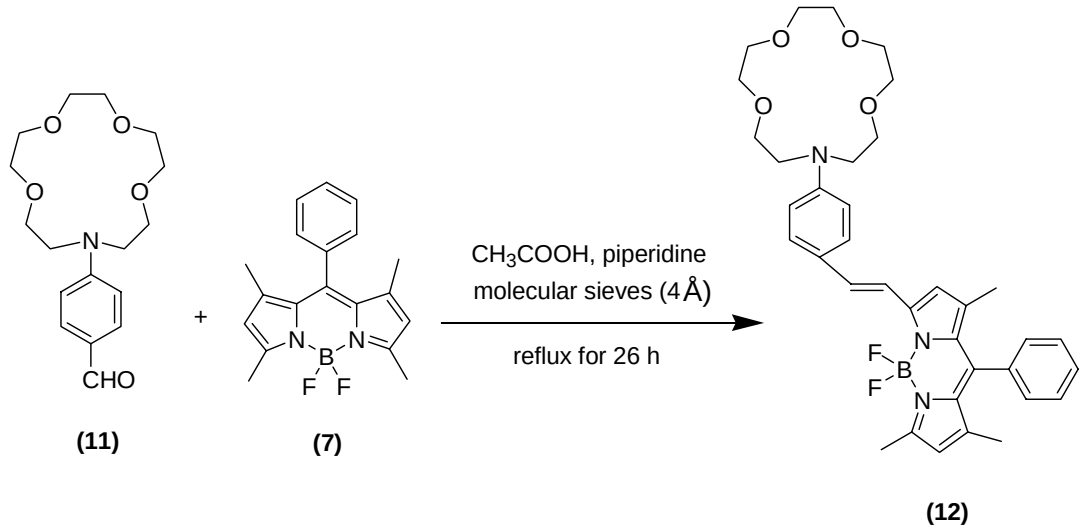

Figure 2.7 Synthesis of 4,4-Difluoro-4-bora-3a,4a-diaza-s-indacene (BODIPY) Dye **(12)**

CHAPTER 3

RESULTS AND DISCUSSION

In this study, we designed and synthesized an unsymetrically substituted BODIPY (4,4-Difluoro-4-bora-3a,4a-diaza-s-indacene) dye series. In these systems, the substituents that are phenylazacrown ethers carrying cation-sensitive group, either monoaza-15-crown-5 or monoaza-18-crown-6, are conjugated to the BODIPY core. We also investigated ion-sensing properties of these BODIPY based dye systems.

BODIPY dyes are highly fluorescent materials that have been used for several different applications. These BODIPY dyes combine the advantages of high molar extinction coefficients ($\varepsilon > 70\ 000\ M^{-1}\ cm^{-1}$) and high fluorescence quantum yields (Φ ca. 0.5-0.8) and can be excited at relatively long wavelengths (ca. 500 nm). These dyes have exceptional spectral and photophysical stability as compared to other fluorescent groups.

BODIPY dyes that are sensitive toward both external physical and chemical triggers provide a versatile basis for the constructions of sophisticated switches that communicate, for instance, through changes in electrochromic and/or fluorescence properties. The design of such BODIPY based systems is important since the

BODIPY core is comparatively readily oxidized and reduced, a prerequisite for fluorescent switches relying on electron or charge transfer (CT), as well as for the generation of stable radical ions that show electrogenerated chemiluminescence upon charge recombination. In these systems, the *meso*-substituted BODIPY chromophore acts as in donor(D)-acceptor(A)-substituted biaryls so that the switching process hardly influences the absorption and emission wavelengths.

In this study, we designed and synthesized more advanced molecular ensembles that generate signal changes by substrate interaction at a site conjugated to the BODIPY core. The molecular sensors that we synthesized are ones of the first examples of an unsymmetrically substituted BODIPY dyes with an analyte-responsive receptor in the polymethinic part of the chromophore. In our systems, the analyte-sensitive group is either monoaza-12-crown-4 or monoaza-15-crown-5 that plays also the role of an electron donor groups because of N atom they have. Having the strong and analytically valuable proton-induced effects on the absorption and emission behaviour of the amino-substituted BODIPY derivatives, we examined the photophysical changes of the dyes we synthesized upon complexation to the some metal cations in acetonitrile in order to test their possible application as fluorescent probes. The crowned BODIPY dyes presented here are examples for very efficient CT (charge transefer) systems. In these systems coordination to the nitrogen donor atom of the receptor not only leads to changes in fluorescence intensity and lifetime but also provides additional information via spectral shifts in both absorption and emission.

3.1 Synthesis and Photophysical Properties of BODIPY Dye (8)

We followed three steps for the synthesis of BODIPY dye **(8)** which is shown in Figure 3.1. In the first step, 18-membered lariat azacrown ether, that is phenyl substituted, was synthesized by cyclization of 2-[(2-Hydroxy-ethyl)-phenyl-amino]-ethanol **(1)** with tetra(ethylene glycol)di-*p*-tosylate **(2)**. The yield was much lower than that expected because of difficulties we had in purification. Then 16-Phenyl-1,4,7,10,13-pentaoxa-16-aza-cyclooctadecane **(3)** that was obtained in first step was formylated with Vilsmeier and Haack reaction. The appearance of the aldehyde proton at δ 9.68 ppm and the disappearance of the peak of proton at the *para*-position of the phenyl at δ 7.28 in the ^{1}H-NMR spectrum show a successful reaction. Finally, the formyl substituted compound **(4)** was reacted with 4,4-Difluoro-4-bora-3a,4a-diaza-*s*-indacene (BODIPY) and the desired final product that is functionalized boron-dipyrromethane dye was obtained.

After synthesis of the BODIPY dye **(8)**, we investigated the photophysical behaviour of upon complexation with some metal cations and proton. In spectrometric measurements acetonitrile was used as solvent, because the BODIPY dyes we synthesized are the intrinsically donor-acceptor-substituted fluoroionophores (ICT probes) that show strong solvent-dependent behavior. In a nonpolar solvent, such as hexane, emission occurs only from a LE (locally excited) state, whereas in a more polar solvent, such as acetonitrile, an ultrafast excited-state charge-transfer reaction from the amino donor to the basic fluorophore takes place. This results in strong quenching of the LE emission and appearance of a bathochromically shifted emission from a lower lying CT state, both fluorescence quantum yields being low.

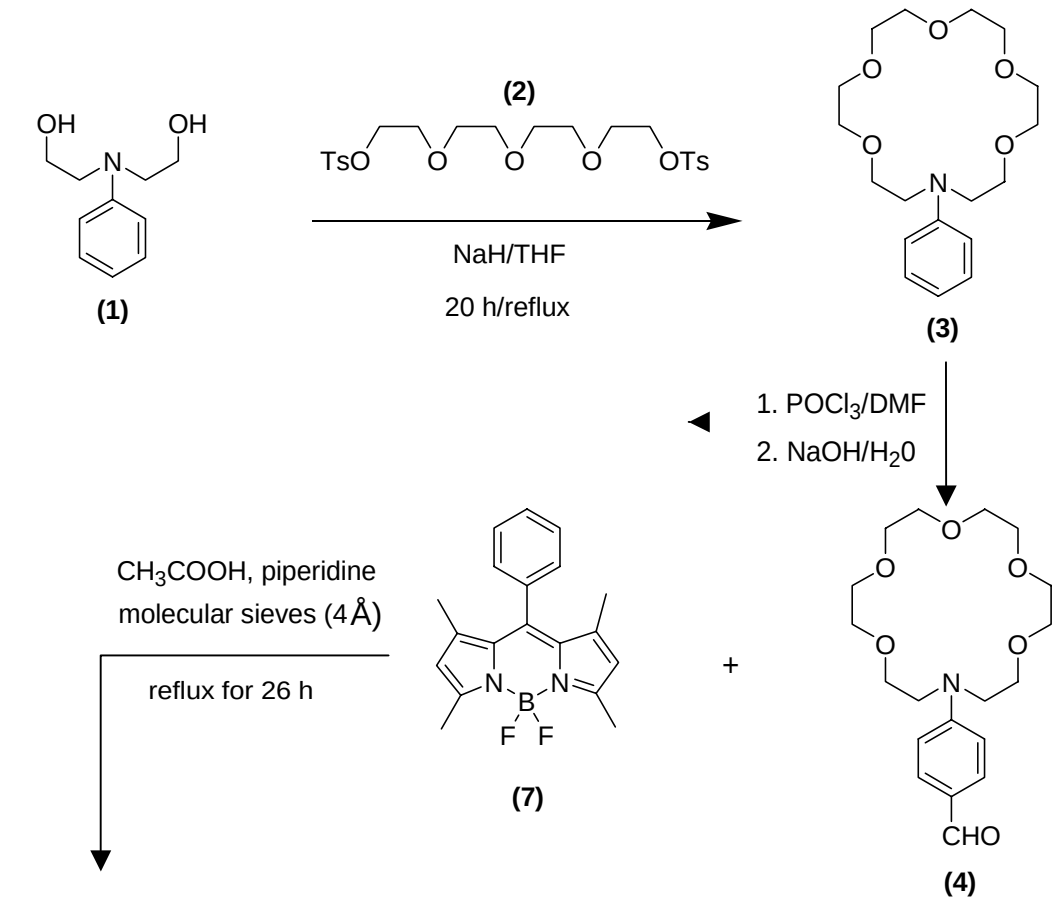

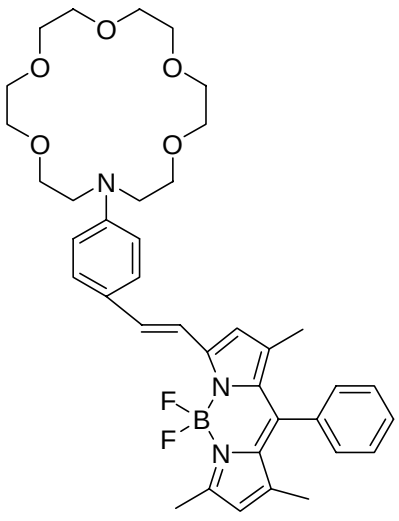

(8)

Figure 3.1 Reaction series leading to BODIPY dye **(8)**

The efficient nonradiative deactivation process can be utilized to construct a very efficient molecular switch. Protonation as well as complexation blocks the CT process and switches on the LE emission again; i.e., a strong increase in LE fluorescence quantum yield and lifetime with very large fluorescent enhancement factors.

Figure 3.2 is the absorption spectra of the complexes with Na^{+}, K^{+}, Ca^{2+}, Zn^{2+}, Cd^{2+}, proton and the free ligand BODIPY dye **8** in acetonitrile.

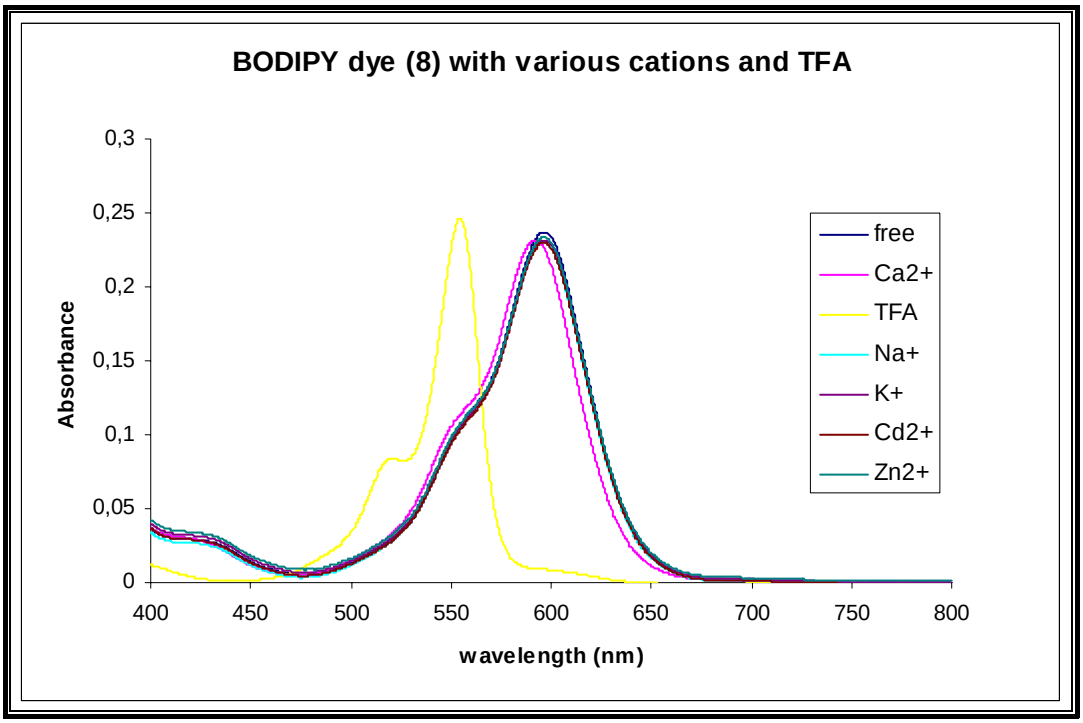

Figure 3.2 Absorption spectra of BODIPY dye **8**, **8**-(metal cations) and **8**-TFA (Trifluoroacetic acid) in acetonitrile. Ligand conc. = 2.8×10^{-5} M, cation conc. = 1.0×10^{-2} M, TFA conc. = 6.5×10^{-2} M.

There is no shift for the Na^{+}, K^{+}, Zn^{2+}, Cd^{2+}, whereas there is blue-shift 4 nm and 42 nm compared to the ligand for complexation with Ca^{2+} and proton respectively

as expected, because when the nitrogen atom in crown ether playing the role of electron donor interacts with a cation or proton, the latter reduces the electron-donating character of this atom; owing to the resulting reduction of conjugation, a blue shift of the absorption spectrum is expected.

The effect of proton binding on the emission spectrum is shown in Figure 3.3. As can be deduced from the figure, protonation drastically alters the electron-donating properties of the crown nitrogen and consequently "switches off" any charge transfer interaction, and that leads to a blue shift of the emission band about 108 nm and 24-fold enhancement of the emission intensity at 565 nm.

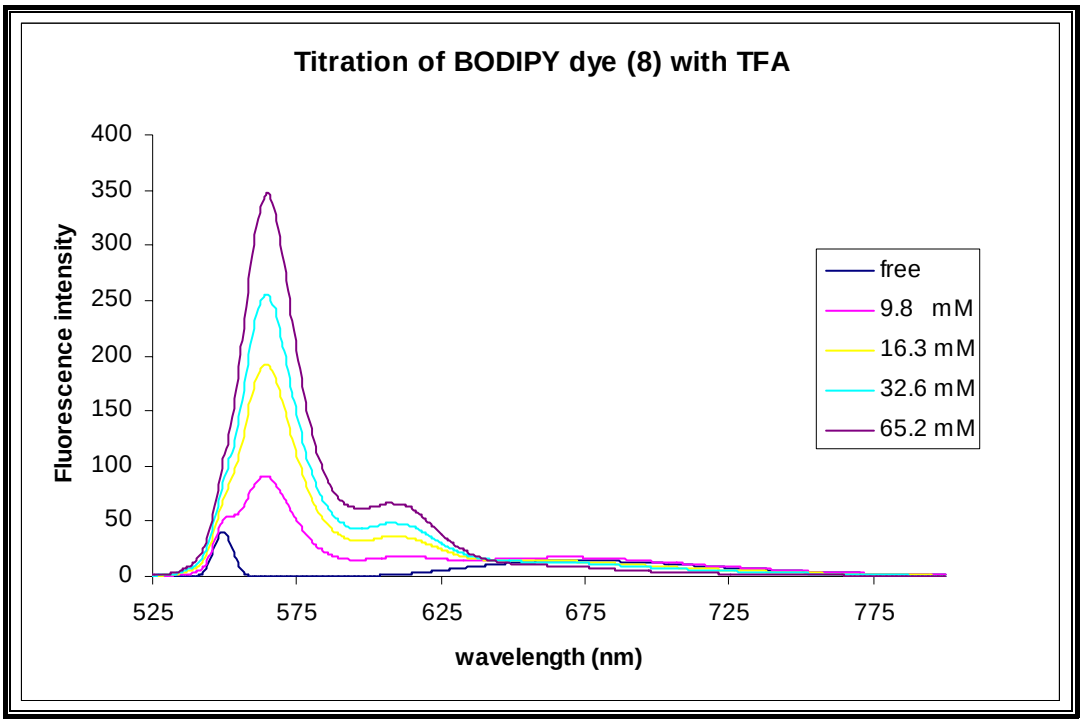

Figure 3.3 Emission spectrum of BODIPY dye **8**, as a function of increasing TFA (Trifluoroacetic acid) concentration in acetonitrile. The small peak at 548 nm is due to scattering.

The complexation-induced effects of metal cations on the emission spectra are shown in Figure 3.4. It can be concluded from the figure that only the complexation of the Ca^{2+} ion leads to FEF (fluorescence enhancement factor) and blue-shift about 13 nm compared to free ligand, which is an unexpected result showing that BODIPY dye **(8)** displays considerably higher affinity for calcium than potassium, despite the fact that 18-crown-6 macrocycles are tailored for the potassium ion.

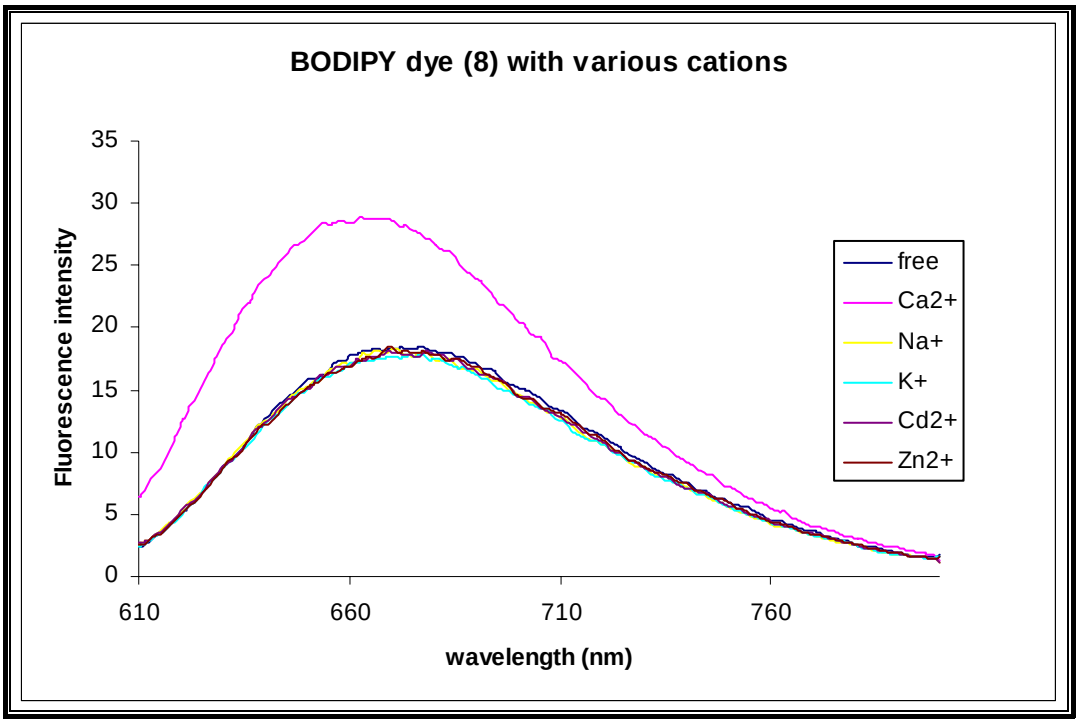

Figure 3.4 Emission spectra of free ligand **8** and **8**-(metal cations) in acetonitrile. Ligand conc. = 1.9×10^{-5} M, metal ion conc. = 1×10^{-2} M, λ_{exc} = 600 nm.

This result may be caused from a conformationally constrained or reduced cavity size, which cause the orientation of the metal cations to one side of the

macrocyclic cavity-remote from nitrogen atom-and coordinated to the oxygen atoms of the crown ether. This accounts for the smaller enhancement of the fluorescence intensity because the inhibition of the nonradiative deactivation pathway can only be achieved by effective coordination of the metal ion to the crown nitrogen.

The effect of calcium ion binding on the fluorescence intensity enhancement with increasing the concentration of calcium metal ion is also shown in Figure 3.5. There is enhancement of the emission intensity at 666 nm from 0 to 7.00 mM.

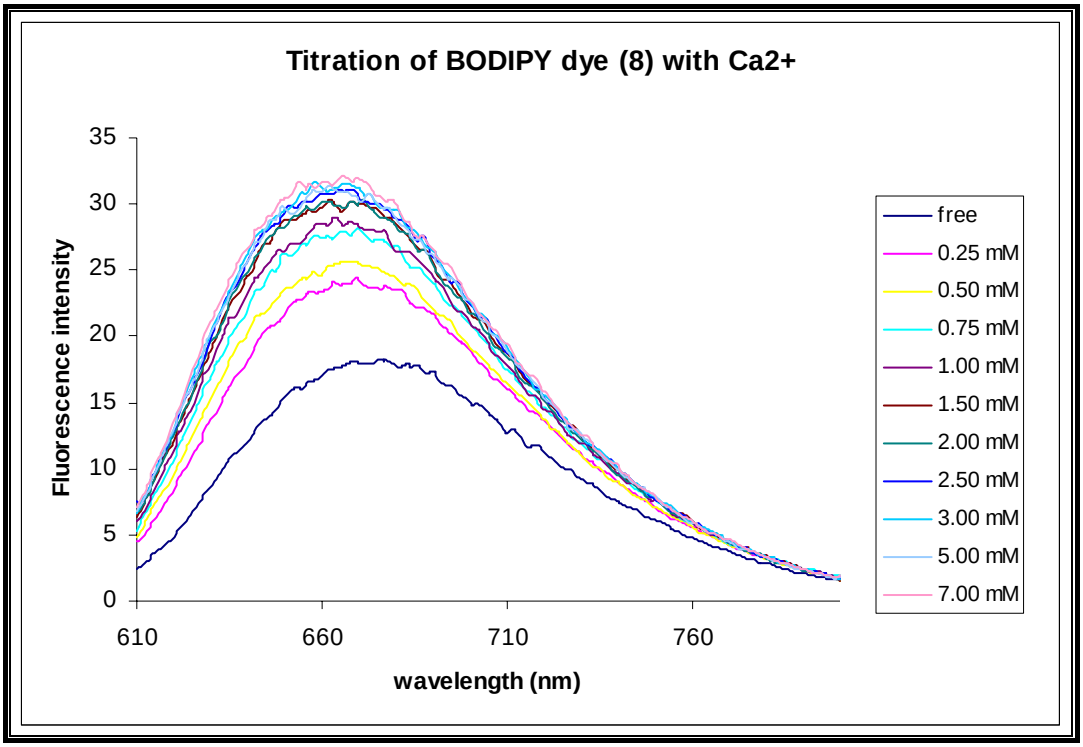

Figure 3.5 Emission spectrum of BODIPY dye **8** in response to increasing calcium ion concentration. Excitation wavelength is 600 nm. The acetonitrile solution is 1.9×10^{-5} M in BODIPY dye **8**. The concentration of calcium perchlorate tetrahydrate is varied from 0 to 7.00 mM.

3.2 Synthesis and Photophysical Properties of BODIPY Dye (12)

We followed three steps for the synthesis of BODIPY dye **(12)** as in the synthesis of BODIPY dye **(8)**, Figure 3.6. In the first step, 15-membered lariant azacrown ether **(10)** that is phenyl substituted was synthesized by cyclization of 2-[(2-Hydroxy-ethyl)-phenyl-amino]-ethanol **(1)** with tri(ethylene glycol)di-*p*-tosylate **(9)**. Then by using Vilsmeier and Haack reaction we formylated the compound **(10)**. Finally, the formyl substituted compound **(11)** was reacted with 4,4-Difluoro-4-bora-3a,4a-diaza-*s*-indacene (BODIPY) and the desired final product that is functionalized boron-dipyrromethane dye **(12)** was obtained.

Spectrophotometric studies of this dye have given us the same results with the dye **(12)**. Figure 3.7 illustrates the blue-shifts by protonation and upon binding of calcium metal ion in absorbance spectrum that is the indicative of an intramolecular CT process. Compared to the ligand there is blue-shift of 5 nm and 44 nm for complexation with Ca^{2+} and proton, respectively.

The increase of the emission intensity as a function of increasing TFA (trifluoroacetic acid) concentration, which is caused from drastically altering of the protonation the electron-donating properties of crown donor nitrogen atom, is shown in Figure 3.8. The interaction leads to blue shift of the emission band about 115 nm and 41-fold enhancement of the emission intensity at 564 nm. The fluorescence enhancement factor is higher in dye **(12)** than that in dye **(8)**, since in dye **(8)** there are five electronegative oxygen atoms that affect the proton, on the other hand dye **(12)** has four oxygen atoms. Therefore, in dye **(12)** the protonation affects the crown nitrogen much higher compared to that in dye **(8)**.

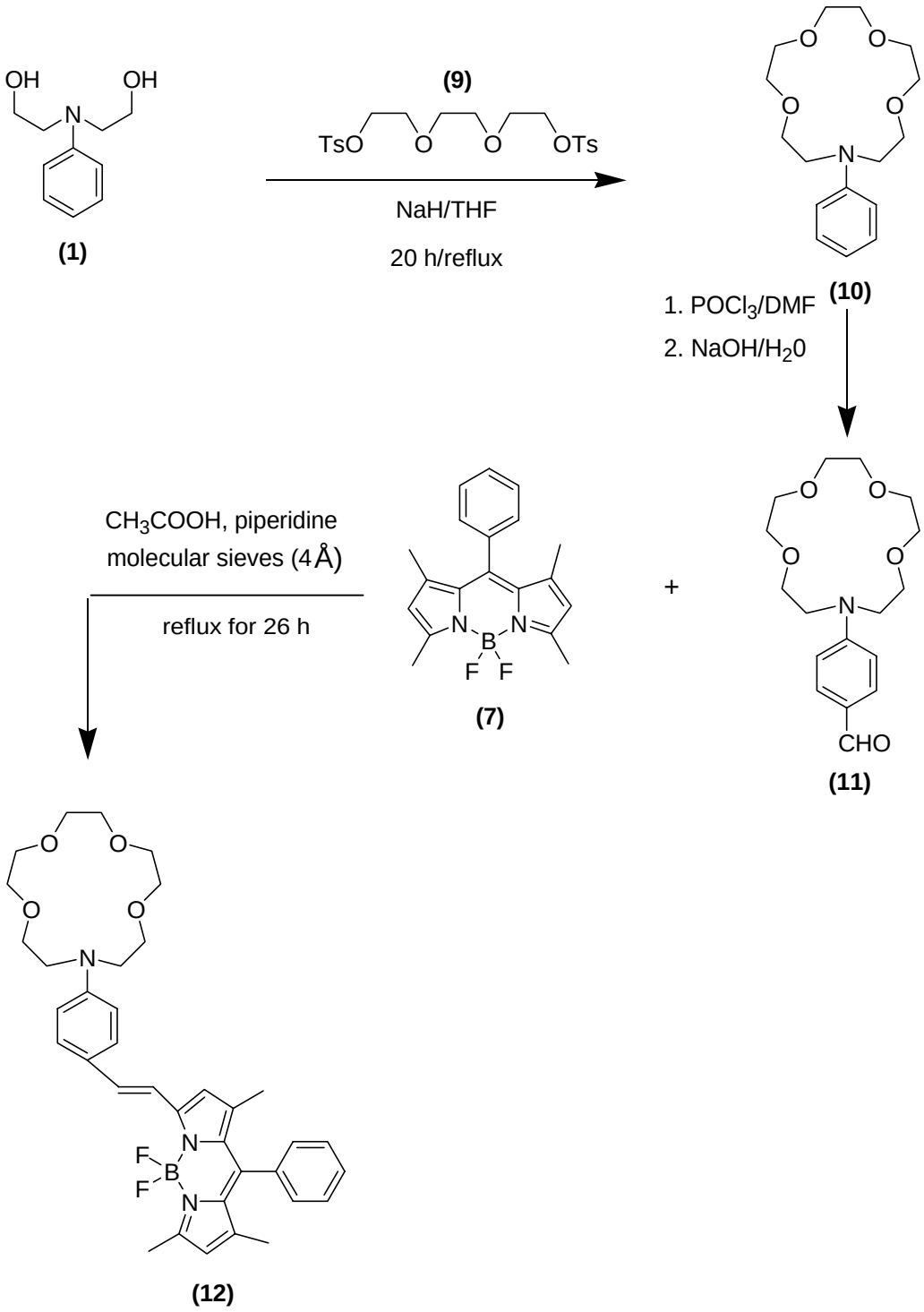

Figure 3.6 Reaction series leading to BODIPY dye **(12)**.

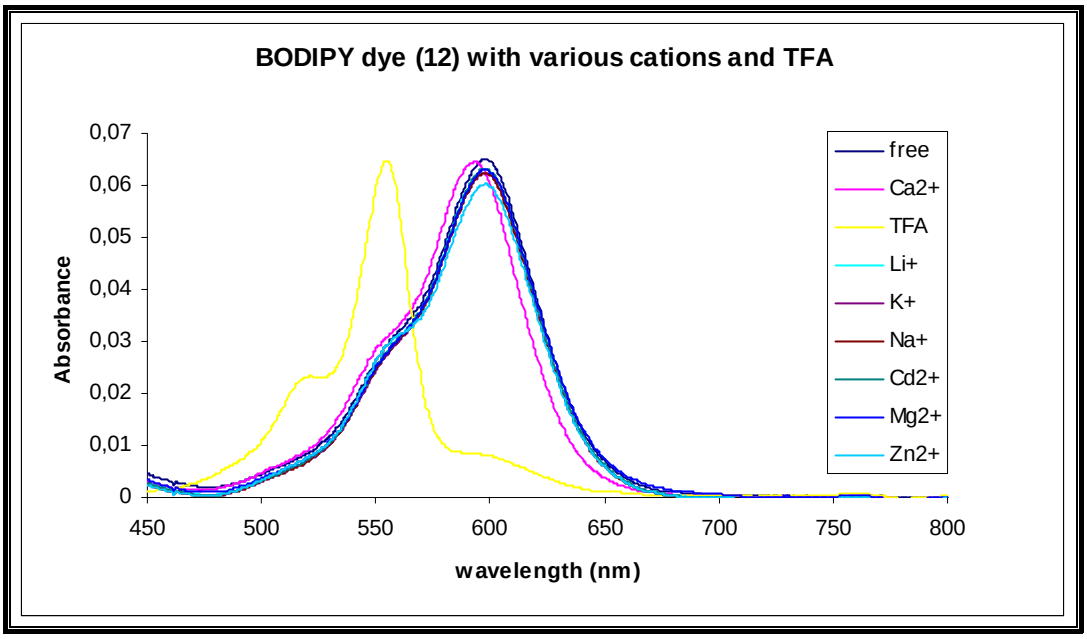

Figure 3.7 Absorption spectra of BODIPY dye **12**, **12**-(metal cations) and **12**-TFA (Trifluoroacetic acid) in acetonitrile. Ligand conc. = 4.7×10^{-7} M, cation conc. = 1×10^{-2} M, TFA conc. = 6.5×10^{-2} M.

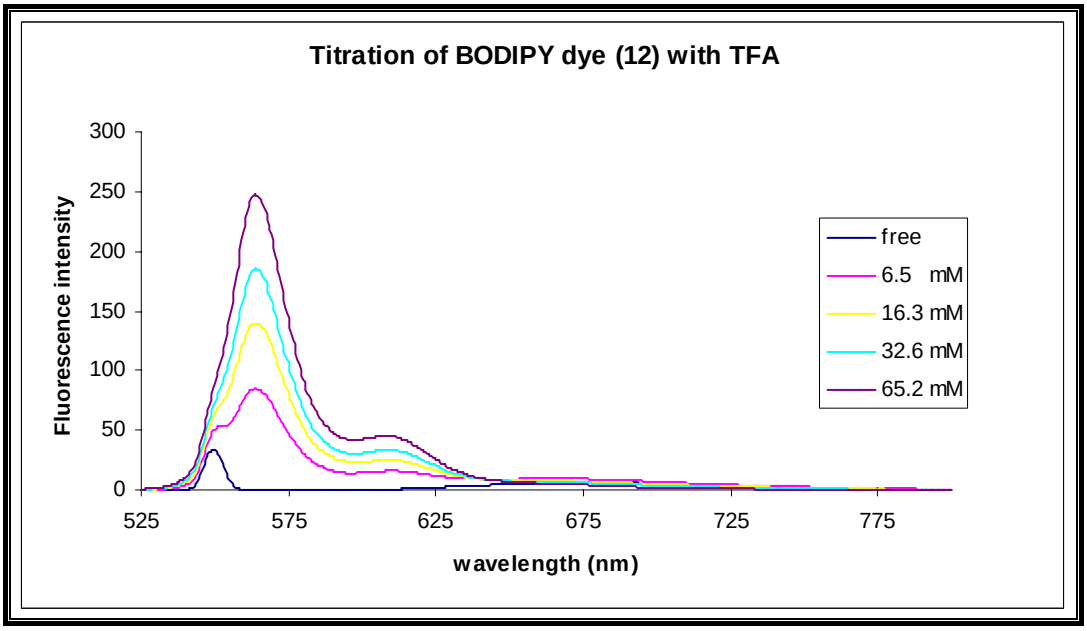

Figure 3.8 Emission spectra of BODIPY dye **12,** as a function of increasing TFA (trifluoroacetic acid) concentration in acetonitrile. The small peak at 550 nm is due to scattering.

The calcium metal ion sensing property of the dye **(12)** and changes in fluorescence intensity upon addition of different calcium metal ion concentrations are shown in Figure 3.9 and Figure 3.10, respectively. It can be concluded from these figures that binding of the cation to the crown ether moiety suppresses the charge transfer process owing to electrostatic interaction between the positively charged cation and the nitrogen electron donor atom, which cause fluorescence enhancement and the 15-nm-blue-shift. The selective complexation of the calcium metal ion can be explained by the cation size and the diameter of the crown moiety as well as the charge density of the cation. The reason for why the other cations do not give any fluorescence enhancement can be explained again by conformationally constrained or reduced cavity size. These cations are supposed to be coordinated mainly by the four crown oxygen and one or two solvent molecules.

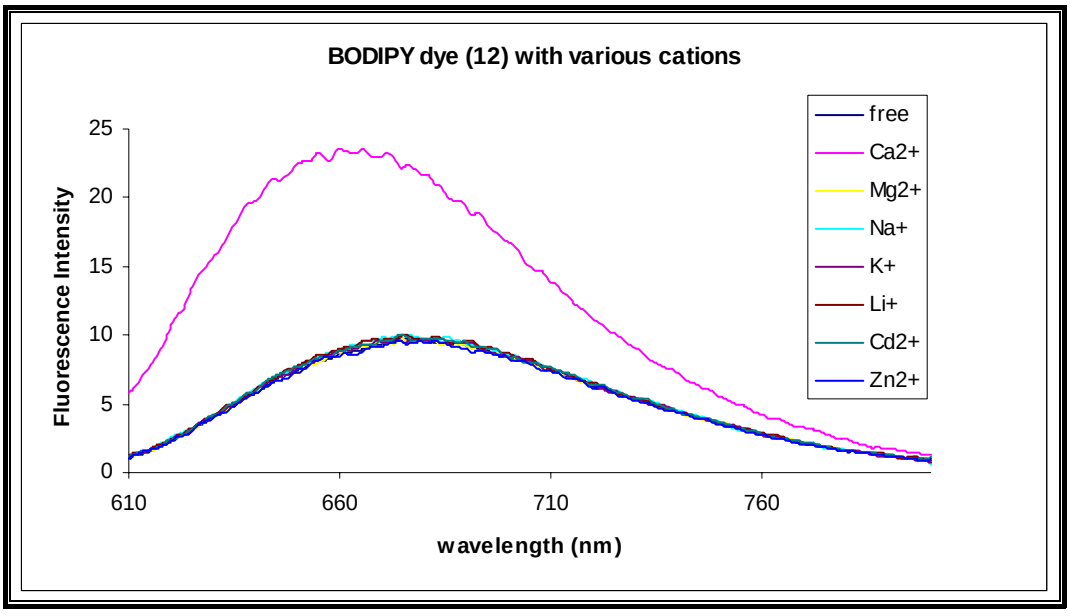

Figure 3.9 Emission spectra of free ligand **12** and **12**-(metal cations) in acetonitrile. Ligand conc. = 2.4×10^{-7} M, metal ion conc. = 1×10^{-2} M, λ_{exc} = 600 nm.

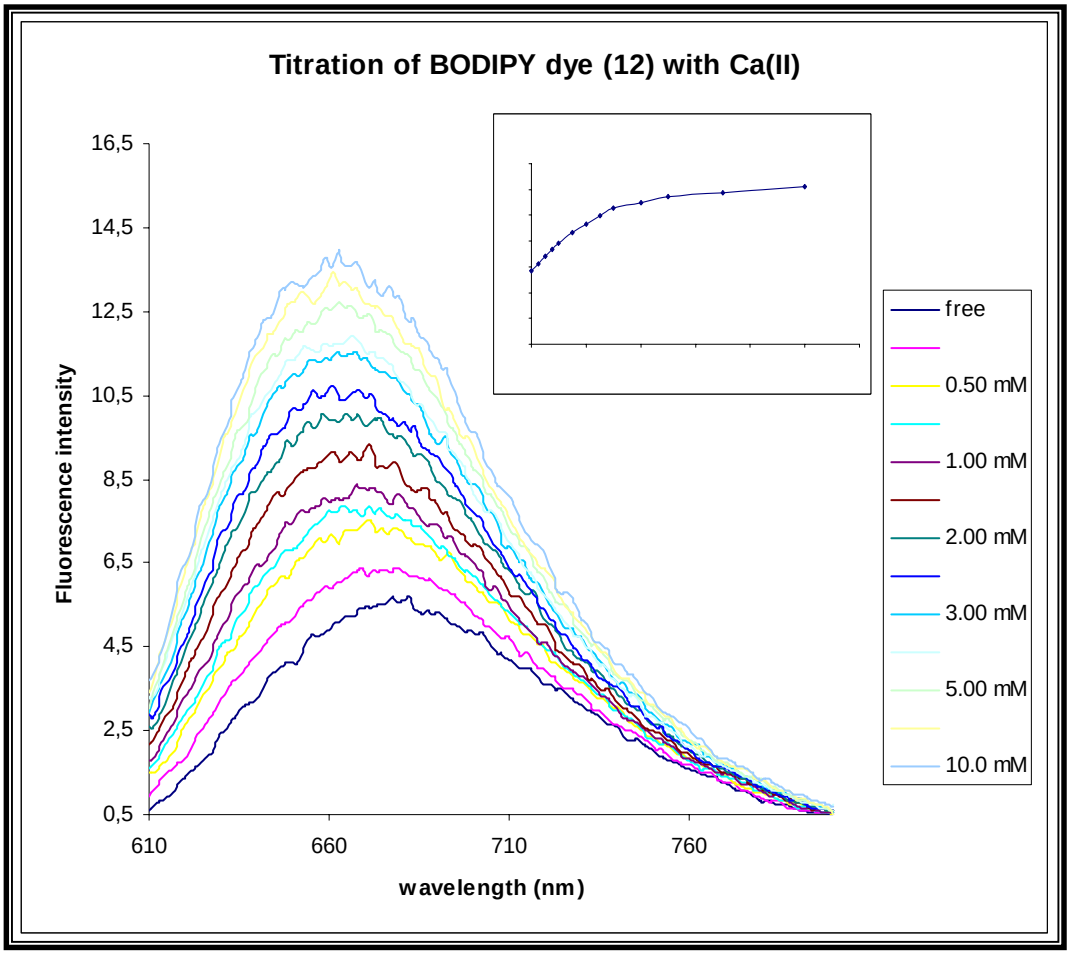

Figure 3.10 Emission spectra of BODIPY dye **12** in response to increasing calcium ion concentration in acetonitrile. Ligand conc. = 2.4×10^{-7} M, excitation at 600 nm. The concentration of calcium perchlorate tetrahydrate is varied from 0 to 10.0 mM. Inset shows the increase in the intensity with respect to Ca^{2+} metal ion concentration, emission max is 682 nm.

CHAPTER 4

CONCLUSION

This study covers the synthesis and ion sensing properties of a series of novel boradiazaindacene dyes.

The molecular sensors that we synthesized in this study are ones of the first examples of an unsymetrically substituted boradiazaindacene dyes with an analyte-responsive receptor in the polymethinic part of the chromophore. The extension of the conjugation over the pyrrole ring shifts the absorption and emission to longer wavelength in our systems. The boradiazaindacene dyes presented here are examples for efficient CT (charge transfer) systems that can be transferred to LE (locally excited) systems by stable calcium metal ion complexation or protonation in polar acetonitrile.

Thus, with these dyes, we present a new design concept for sensitive probes for calcium metal ion showing absorption and fluorescence changes in the red/NIR. Especially considering the selective signaling of calcium ions, which is very important biological analyte, one can foresee practical applications in many fields by appropriate derivatization of the compounds developed by us. Further research in this area will continue in our lab.

REFERENCES

[1] Lehn, J.-M., *Angew. Chem*. **1988**, *100*, 91.

[2] Lehn, J.-M., *Angew. Chem. Int. Ed. Engl.* **1988**, *27*, 89.

[3] Lehn, J.-M., *Supramolecular Chemistry – Concepts and Perspectives*, VCH, Weinheim, **1995**.

[4] Lehn, J.-M, *Science*, **1985**. *227*, 849.

[5] Vögtle, F., Supramolekulare Chemie, Teubner, Stuttgart, **1989**, p 6.

[6] Czarnik, A. W., "Supramolecular Chemistry, Fluorescence, and Sensing", Czarnic, A.W. (Ed), ACS Symposium Series 538, *American Chemical Society*, Washingtion, D.C.,**1992**.

[7] http://www.shsu.edu/~chemistry/chemiluminescence/JABLONSKI.html (11.08.2003).

[8] Czarnik, A. W., "Fluorescent Signal Transduction in Molecular Sensors and Dosimeters", Czarnic, A.W. (Ed), ACS Symposium Series 538, *American Chemical Society*, Washingtion, D.C.,**1992**.

[9] Szmacinski, H., Lakowicz, J. R., "Lifetime-Based Sensing Using Phase-Modulation Fluorimetry", Czarnic, A.W. (Ed), ACS Symposium Series 538, *American Chemical Society*, Washingtion, D.C.,**1992**.

[10] Lehn, J.-M., *Struct. Bonding*, **1973**, *16*, 1.

[11] Valeur, B., *Molecular Luminescence Spectroscopy-Methods and Applications, Part 3*, Ed. Schulman, S. G., John Wiley&sons, New York, **1993** pp 25-84.

[12] Tsein, R. Y., "Fluorescent and Photochemical Probes of Dynamic Biochemical Signals insida Living Cells", Czarnic, A.W. (Ed), ACS Symposium Series 538, *American Chemical Society*, Washingtion, D.C.,**1992**.

[13] Minta, A., Tsein, R. Y., *J. Biol. Chem*., **1989,** *264*, 19449.

[14] Tsien, R. Y., Poenie, M., *Trends Biochem*. Sci., **1986**, *11*, 450.

[15] Bright, G. R., Fisher, G. W., Rogowska, J., Taylor, D. L., *Fluorescence Microscopy of Living Cells in Culture Part B, Methods in Cell Biology,* Vol. 30 (Taylor D. L. and Wang, Y. –L., Eds.), pp 157-192. Academic Press, San Diego, **1989**.

[16] Valuer, B., Bourson, Jean, Pouget, J., "Ion Recognition Detected by Changes in Photoinduced Charge or Energy Transfer", Czarnic, A.W. (Ed), ACS Symposium Series 538, *American Chemical Society*, Washingtion, D.C.,**1992**.

[17] Valeur, B., Leray, I., *Coordination Chemistry Reviews*, **2000**, *205*, 3.

[18] Valuer, B., "Fluorescent Probe Design for Ion Recognition" in *Topics in Fluorescence Spectroscopy, Probe Design and Chemical Sensing*, Lakowicz, J. R. (Ed.), Plenum Press, New York, **1994**, **4**, pp 21-48.

[19] Bissell, R. A., de Silva, A. P., Gunaratne, H. Q. N., Lynch, P. L. M., Maguire, G. E. M., Sandanayake, K. R. A. S., *Chem. Soc. Rev*., **1992**, *21*, 187.

[20] Akkaya, E.U., Oğuz, U., *Tetrahedron Letters*, **1997**, *38*, 4509.

[21] Bissell, R. A., de Silva, A. P., Gunaratne, H. Q. N., Lynch, P. L. M., McCoy, C. P., Maguire, G. E. M., Sandanayake, K. R. A. S., *Top. Curr. Chem*, **1993**, *168*, 223.

[22] Bryan, A.J., de Silva, A. P., de Silva, A. S., Rupasinghe, R. A. D. D., *Biosensors*, **1989**, *4*, 169.

[23] de Silva, A. P., de Silva, A. S., Dissanayake, A S., Sandanayake, K. R. A. S., *J. Chem. Soc. Chem. Commun.*, **1989**, 1054.

[24] de Silva, A. P., Sandanayake, K. R. A. S., *J. Chem. Soc., Chem. Commun.*, **1989**, 1183.

[25] Prasanna de Silva, A., de SilvA S. A., *J. Chem. Soc., Chem. Commun*., **1986**,1709.

[26] Fabrizzi, L., Lichelli, M., Pallavicini, P., Sacchi, D., Taglietti, A., *Analyst*, **1996**, *121*, 1763.

[27] Bergonzi, R., Fabrizzi, L., Lichelli, M., Mangano, C., *Coord. Chem. Rev*., **1998**, *170*, 31-46.

[28] Golchini, K., Mackovic-Basic, M., Gharib, S. A., Masilamani, D., Lucas, M. E., Kurtz, I., *Am. J. Physiol*., **1990**, *258*, F438.

[29] Fabrizzi, L., Lichelli, M., Pallavacini P., Perotti, A., Sacchi, D., *Angew. Chem. Int. Ed. Ing.*, **1994**, *33*, 1975.

[30] Fabrizzi, L., Lichelli, M., Pallavacini P., Perotti, Taglietti, A., Sacchi, A., *Chem. Eur. J. 2*, **1996**, 167.

[31] de Silva, A. P., Gunaratne, H. Q. N., *J. Chem. Soc. Chem. Commun*., **1990**, 186.

[32] Aoki, I., Sakaki, T., Shinkai, S., *J. Chem. Soc. Chem. Commun*., **1992**, 730.

[33] Kubo, K., Kato, N., Sakurai, T., *Bull. Chem. Soc. Jpn*., **1997**, *70*, 3041.

[34] Löhr, H.-G., Vögtle, F., *Acc. Chem. Res*., **1985**, *18*, 65.

[35] Fery-Forgues, S., Le Bris, M.-T., Guette', J. P., Valeur, B., *J. Chem. Soc. Chem. Commun.*, **1988**, *5*, 384.

[36] Fery-Forgues, S., Le Bris, M.-T., Guette', J. P., Valeur, B., *J. Phys. Chem*., **1988**, *92*, 6233.

[37] Fery-Forgues, S., Bourson, J., Dallery, L., Valeur, B., *New J. Chem*, **1990**, *14*, 617.

[38] Addleman, R. S., Bennett, J., Tweedy, S. H., Elshani, S., Wai, C. M., *Talanta*, **1998**, *46,* 573.

[39] Crossley, R., Goolamanli, Z., Gosper, J., Sammes, P. G., *J. Chem. Soc. Perkin Trans. 2*, **1994**, 513.

[40] Haugland, R. P., *Handbook of Fluorescent Probes and Research Chemicals, Molecular Probes*, Inc, Eugene, OR, USA.

[41] Bourson, J., Pouget, J., Valuer, B., *J. Phys. Chem.*, **1993**, *97*, 4552.

[42] Kollmannsberg, M., Rurack, K., Resch-Genger, U., Daub, J., *J. Phys. Chem. A*, **1998**, *102*, 10211-10220.

[43] Bergstrőm, F., Mikhalyov, I., Hägglőf, P., Wortmann R., Ny, T., Johansson, L.B.-Å., *Journal of American Chemical Society*, **2001**.

[44] Burghart, A., Kim, H., Welch, M. B., Thoresen, L. H., Reibenspies, J., Burgess, K., *J. Ogr. Chem*, **1999,** *64*, 7813.

[45] Chen, J., Reibenspies, J., Derecskei-Kovacs, A., Burgess, K., *Chem. Commun.*, **1999**, 2501.

[46] Kim, H., Burghart, A., Welch, M.B., Reibenspies, J., Burgess, K., *Chem. Commun.*, **1999**,1889.

[47] Chen, J., Burghart, A., Wan, C.-W., Thai, L., Ortiz, C., Reibenspies, J., Burgess, K., *Tetrahedron Letters*, **2000**, *41*, 2303.

[48] Chen, J., Burghart, A., Derecskei-Kovacs, A., Burgess, K., *J. Org. Chem.*, **2000**, *65*, 2900.

[49] Beer, G., Rurack, K., Daub, J., *Chem. Commun.*, **2001**, 1138.

[50] Coskun, A., Baytekin, B., Akkaya, E. U., *Tetrahedron Letters*, **2003**, *44*, 5649.

[51] Kollmannsberg, M., Rurack, K., Resch-Genger, U., Daub, J., *J. Am. Chem. Soc.*, **2000**, *122*, 968.

[52] Werner, T., Huber, C., Heinl, S., Kollmannsberg, M., Daub, J., Wolfbeis, O. S., *Fresenius J. Anal. Chem.*, **1997**, *539,* 150.

[53] Kollmannsberg, M., Gareis, T., Heinl, S., Breu, J., Daub, J., *Angew. Chem. Int. Ed. Ingl.*, **1997**, *36*, 1333.

[54] Rurack, K., Kollmannsberg, M., Daub, J., *Angew. Chem. Int. Ed.*, **2001**, *40*, 385.

APPENDIX

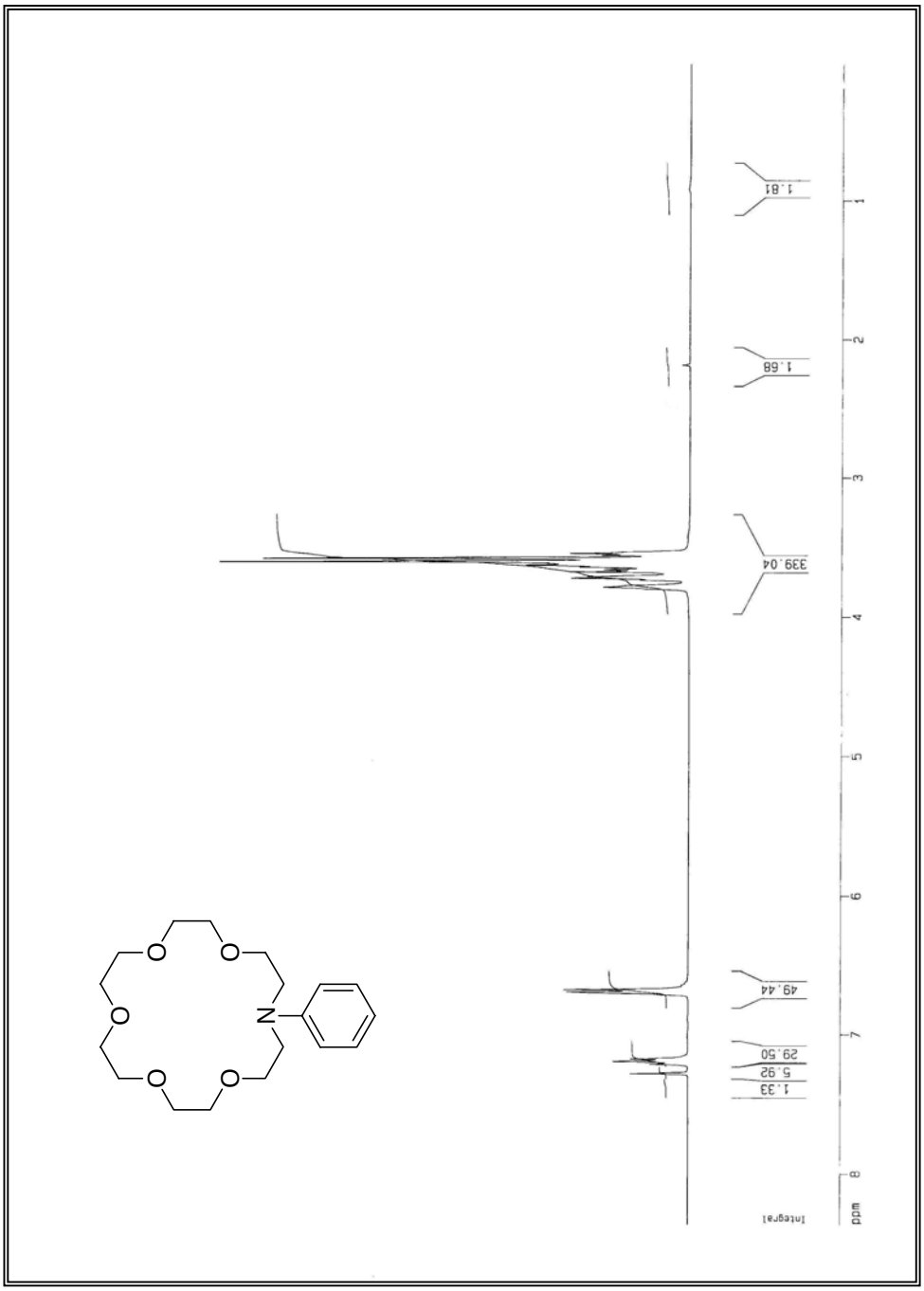

Figure A.1 ^{1}H-NMR spectrum of compound **(3)**.

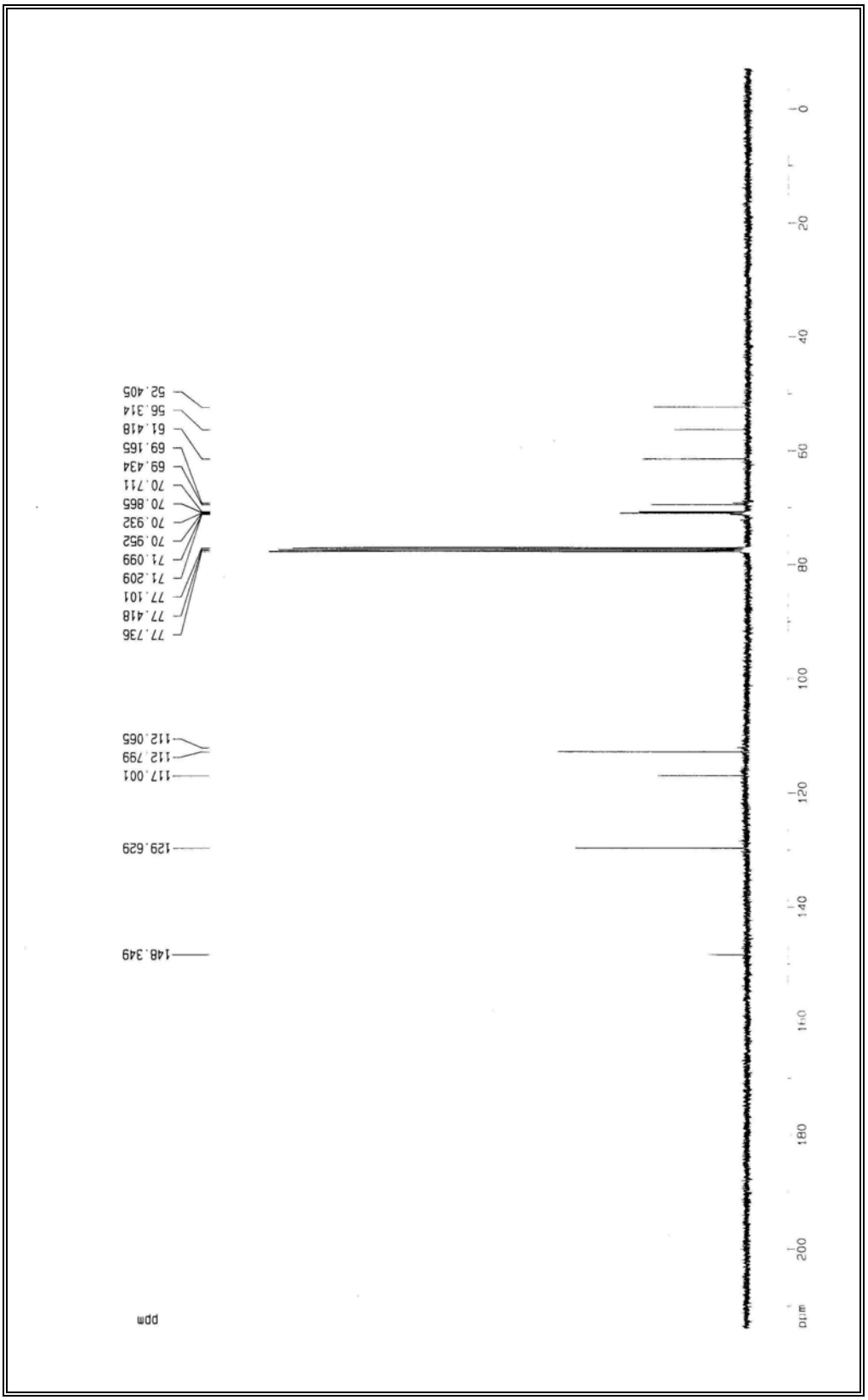

Figure A.2 ^{13}C-NMR spectrum of compound **(3)**.

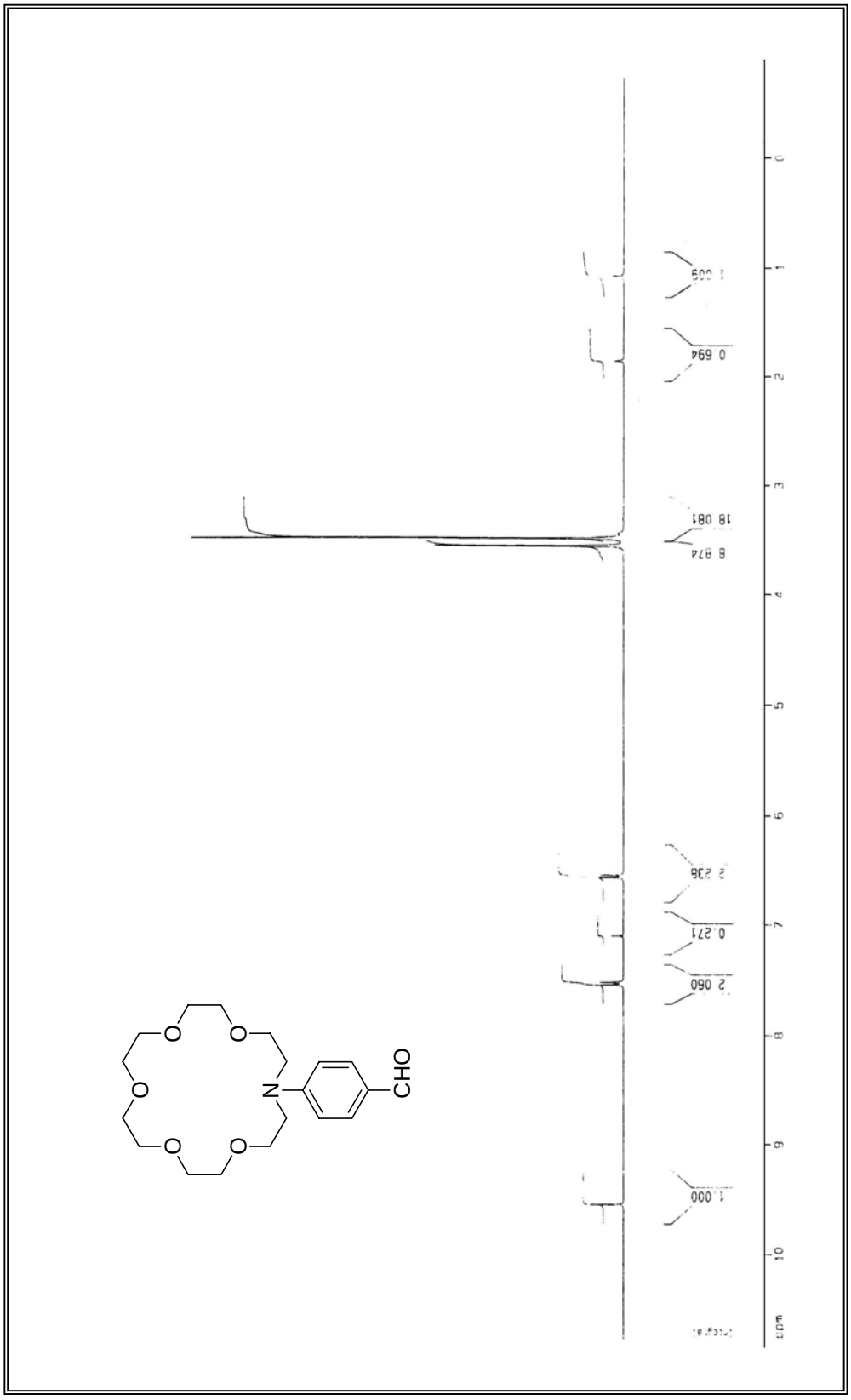

Figure A.3 ^{1}H-NMR spectrum of compound **(4)**.

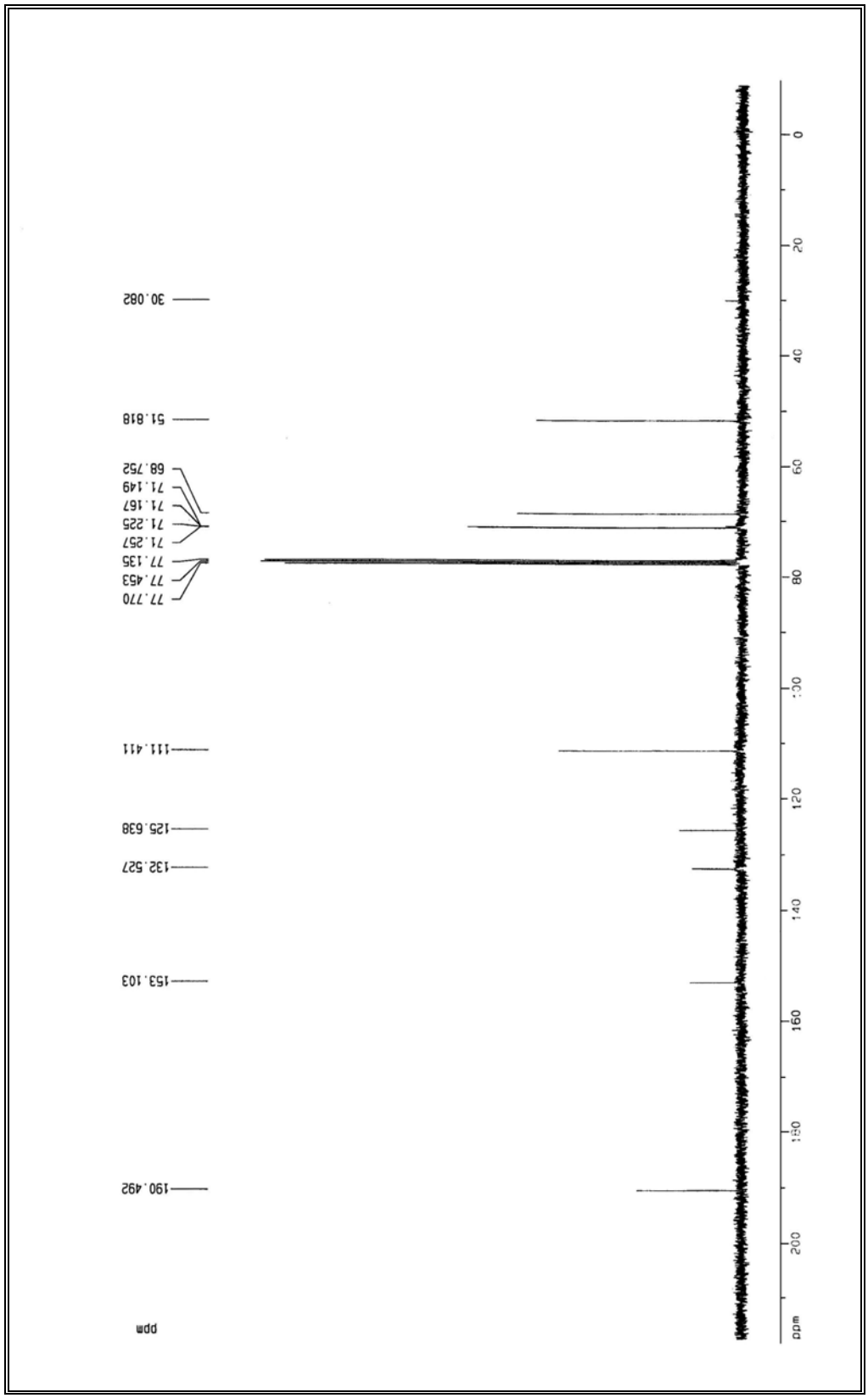

Figure A.4 ^{13}C-NMR spectrum of compound **(4)**.

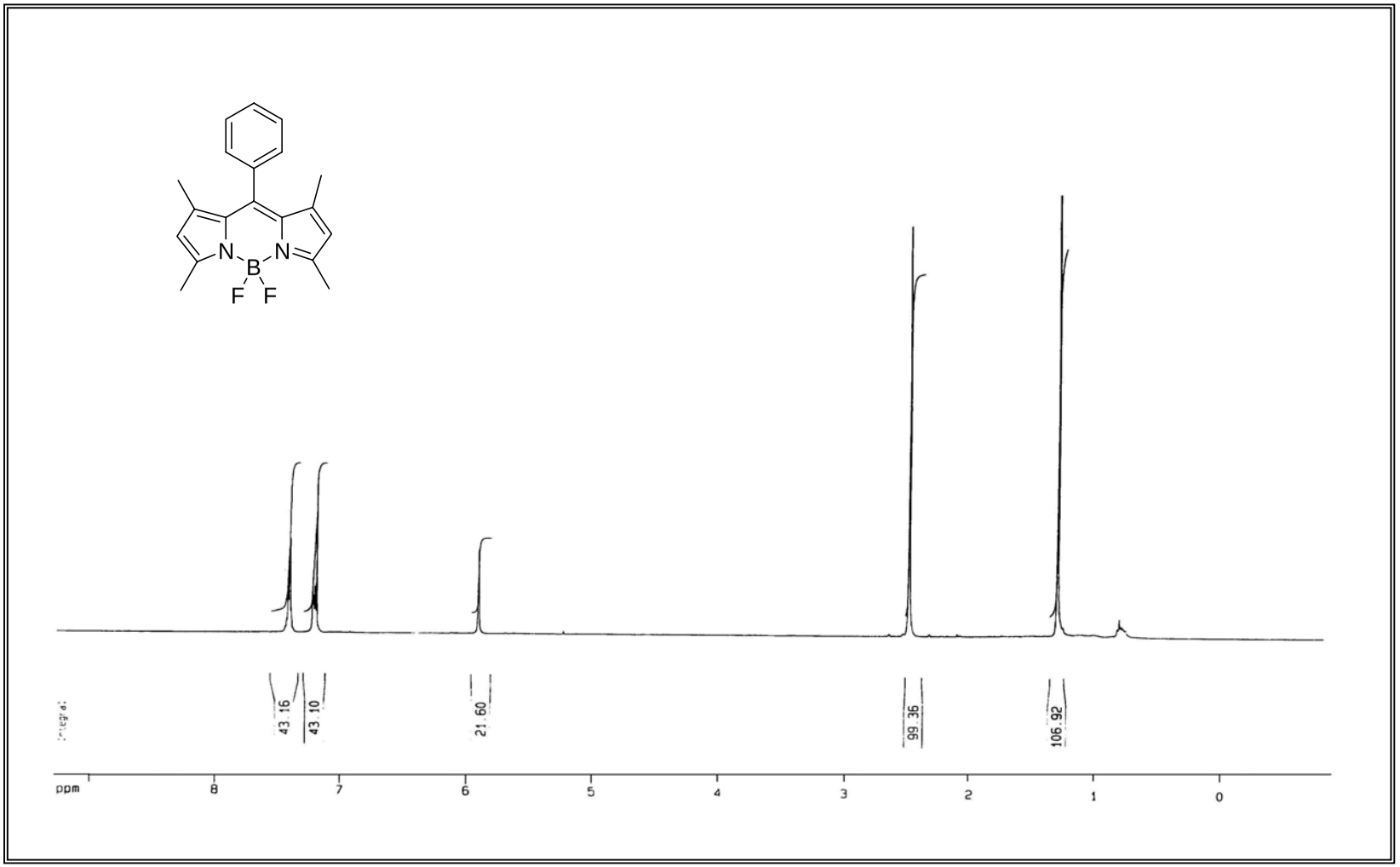

Figure A.5 ^{1}H-NMR spectrum of compound **(7)**.

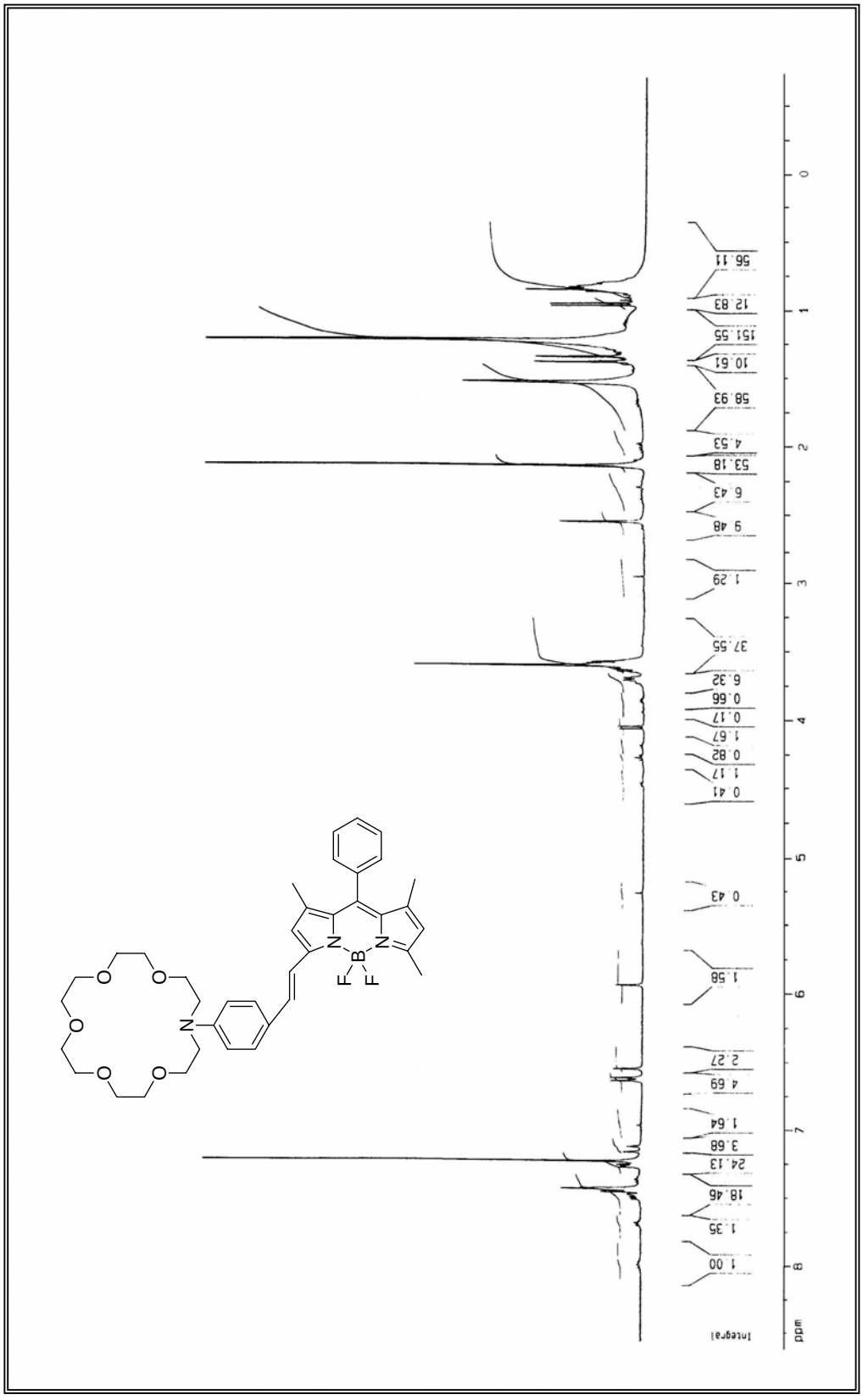

Figure A.6 ^{1}H-NMR spectrum of compound **(8)**.

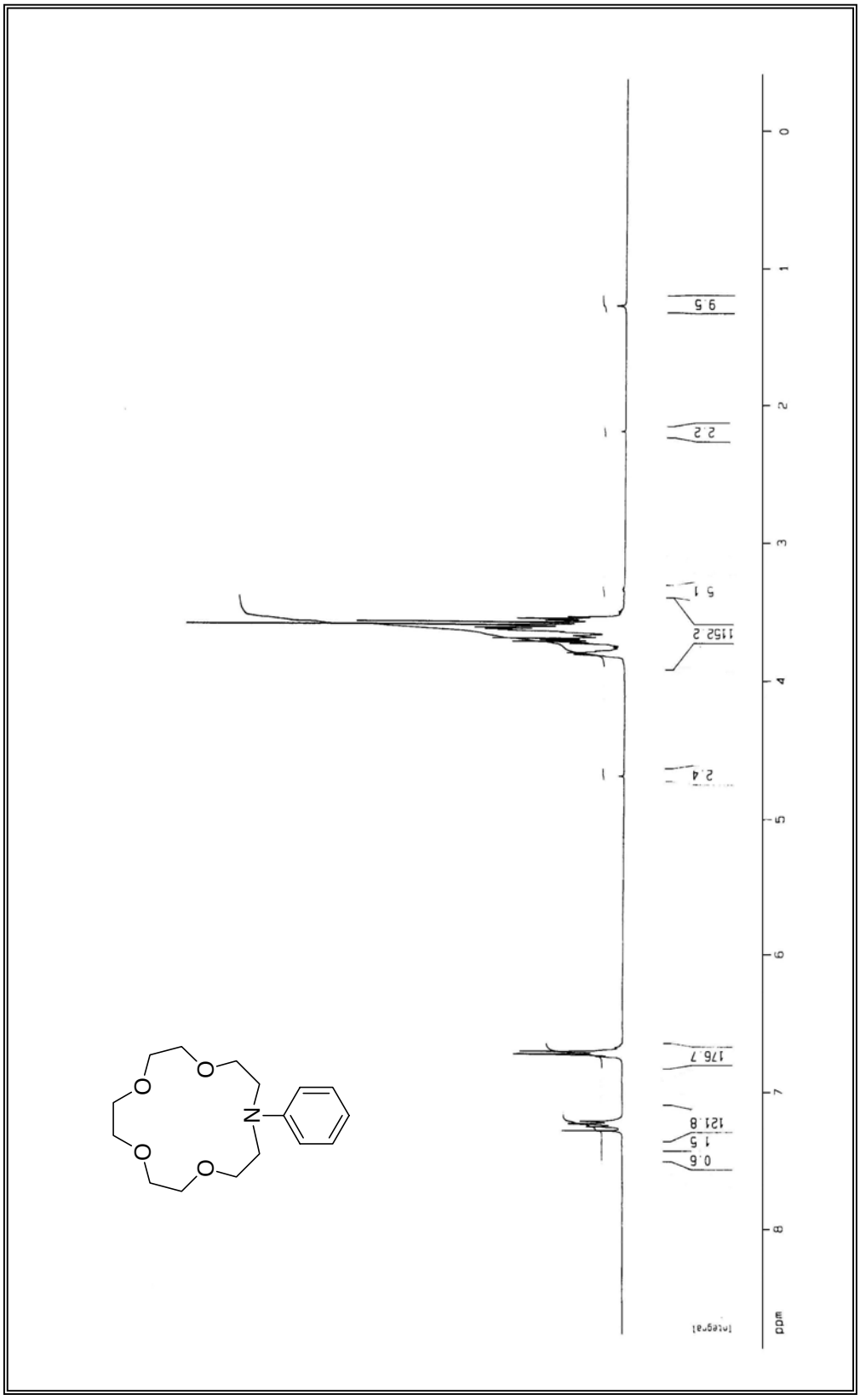

Figure A.7 ^{1}H-NMR spectrum of compound **(10)**.

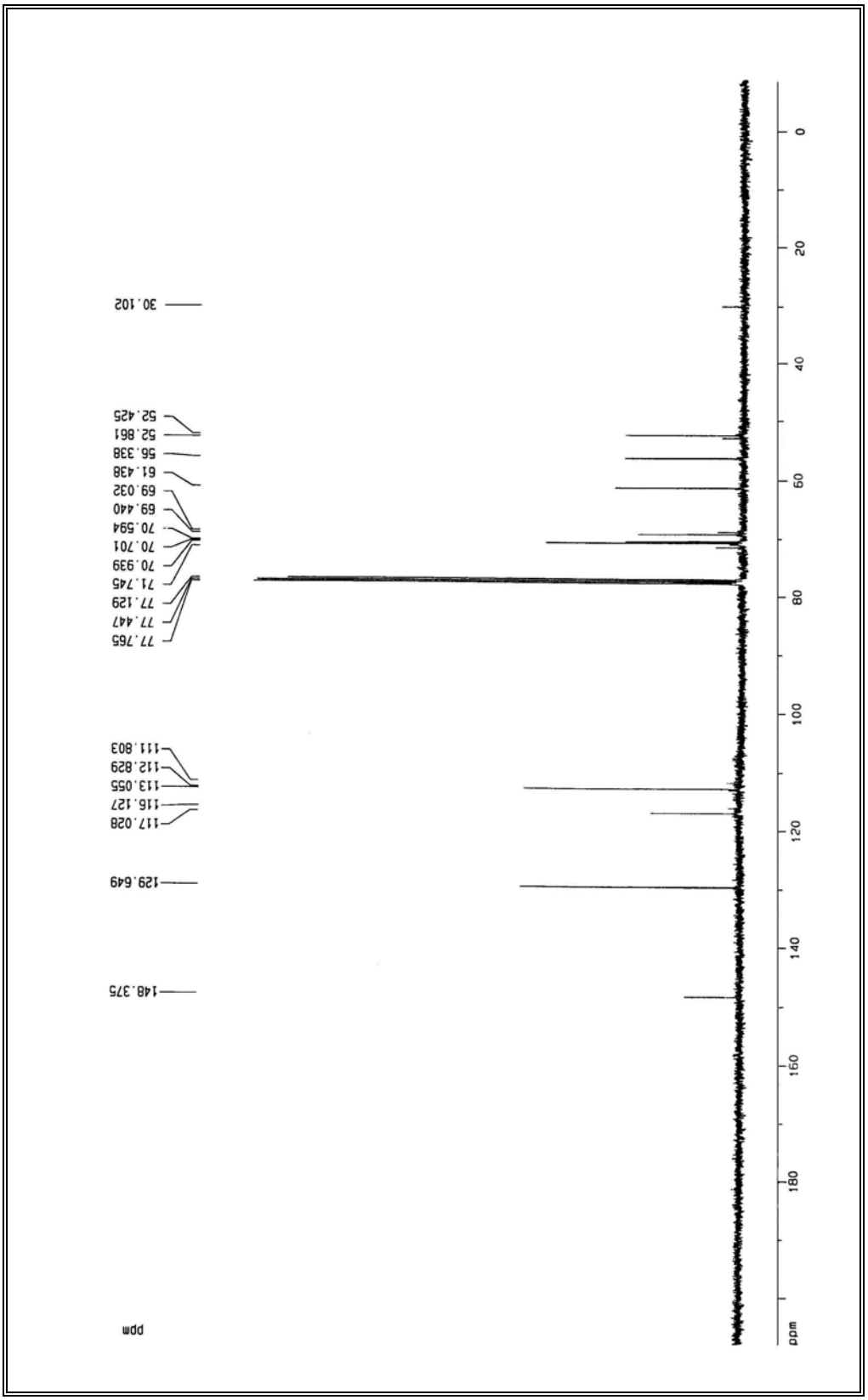

Figure A.8 ^{13}C-NMR spectrum of compound **(10)**.

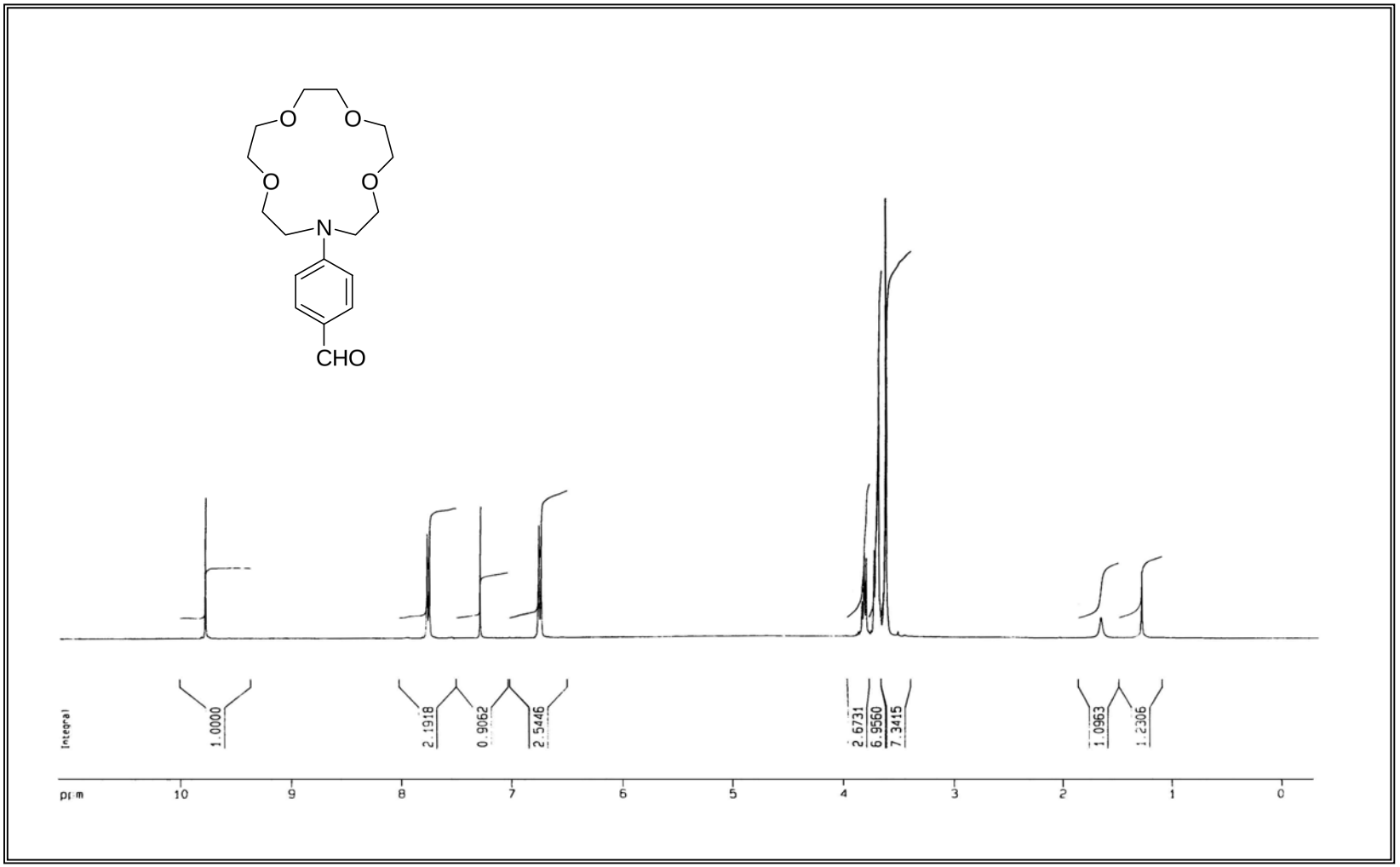

Figure A.9 ^{1}H-NMR spectrum of compound **(11)**.

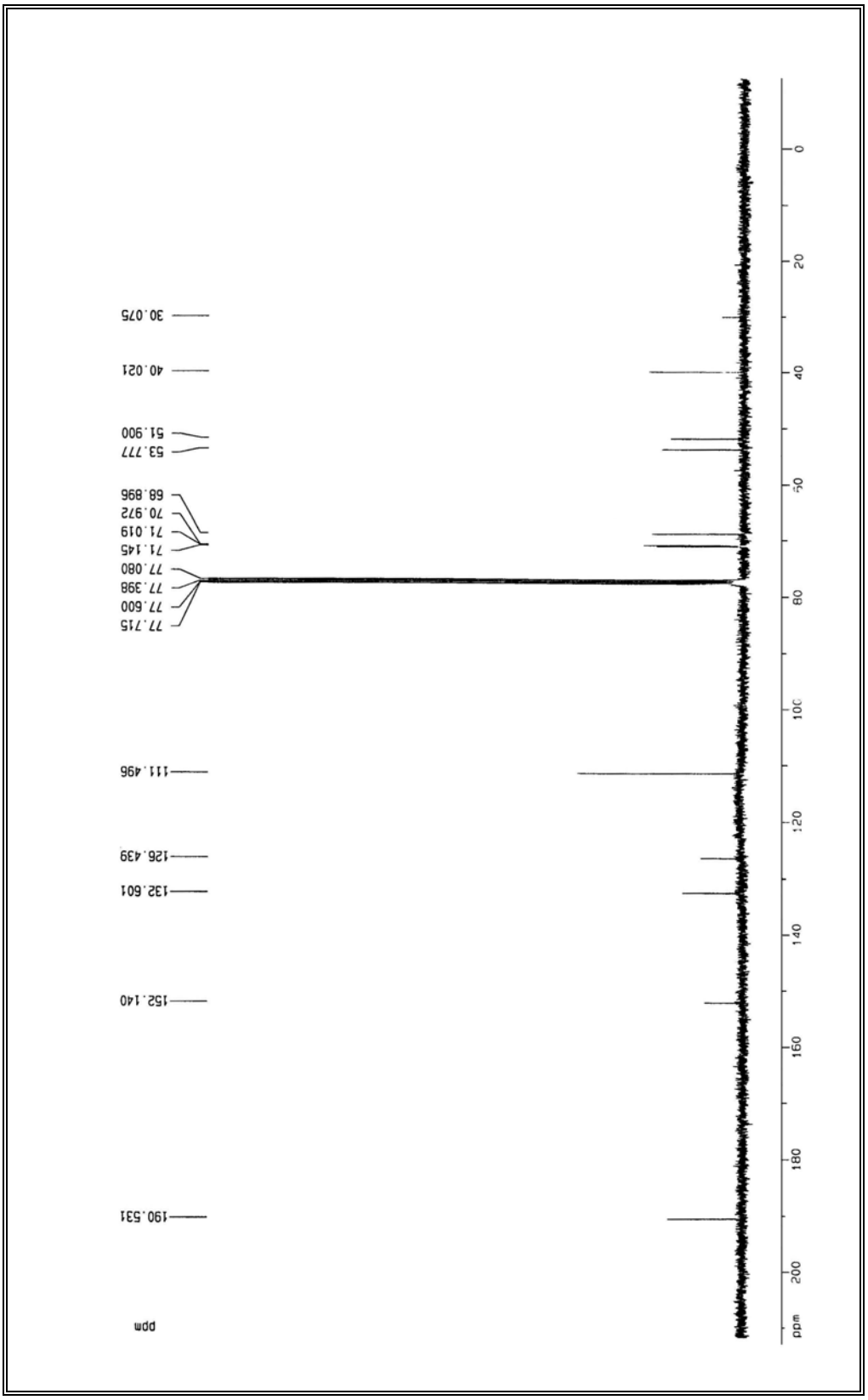

Figure A.10 ^{13}C-NMR spectrum of compound **(11)**.

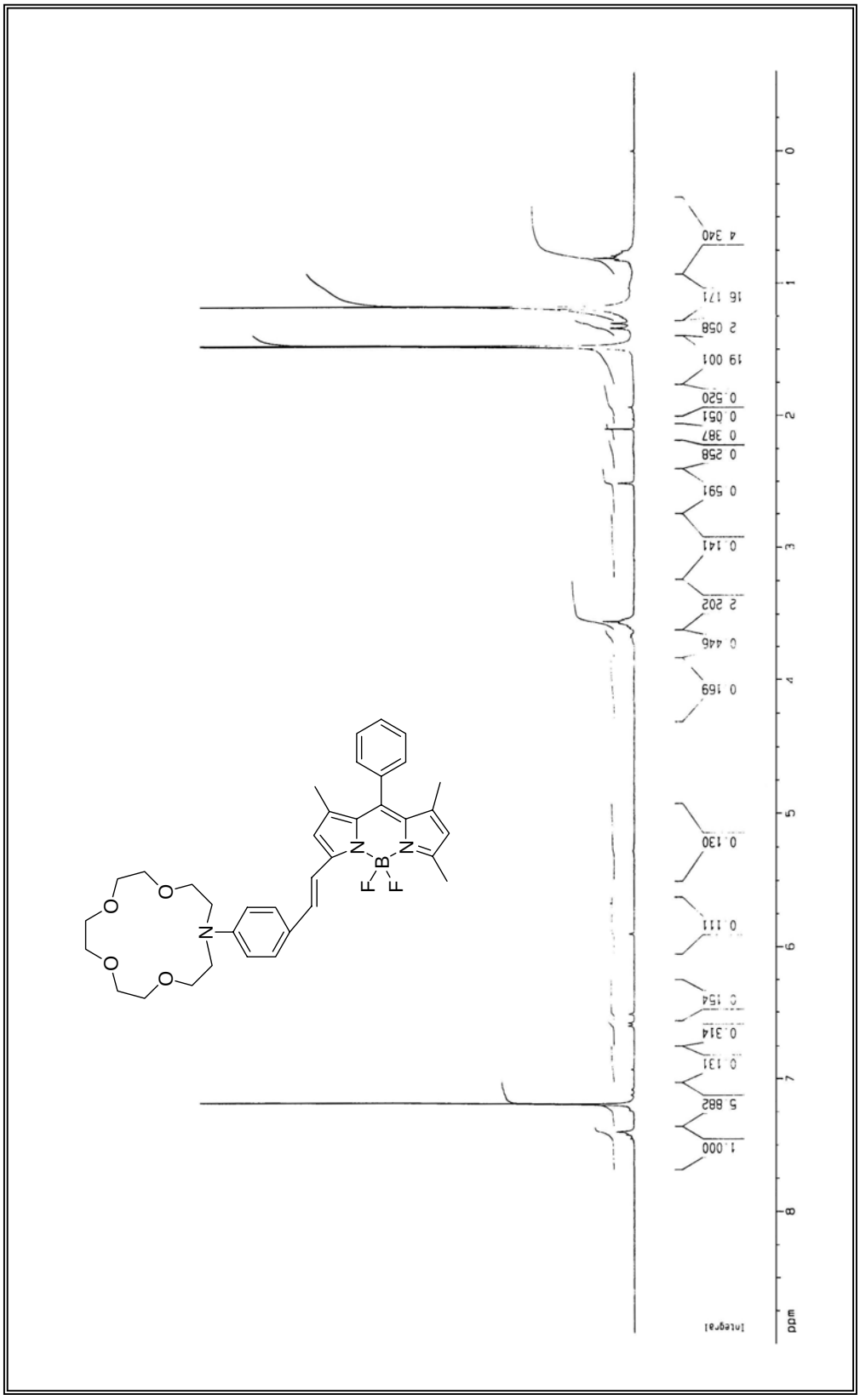

Figure A.11 ^{1}H-NMR spectrum of compound **(12)**.